Development 140, 831-842 (2013) doi:10.1242/dev.088534
© 2013. Published by The Company of Biologists Ltd

Signal transduction by the Fat cytoplasmic domain

Guohui Pan, Yongqiang Feng*, Abhijit A. Ambegaonkar, Gongping Sun, Matthew Huff, Cordelia Rauskolb and Kenneth D. Irvine‡

SUMMARY

The large atypical cadherin Fat is a receptor for both Hippo and planar cell polarity (PCP) pathways. Here we investigate the molecular basis for signal transduction downstream of Fat by creating targeted alterations within a genomic construct that contains the entire *fat* locus, and by monitoring and manipulating the membrane localization of the Fat pathway component Dachs. We establish that the human Fat homolog FAT4 lacks the ability to transduce Hippo signaling in *Drosophila*, but can transduce *Drosophila* PCP signaling. Targeted deletion of conserved motifs identifies a four amino acid C-terminal motif that is essential for aspects of Fat-mediated PCP, and other internal motifs that contribute to Fat-Hippo signaling. Fat-Hippo signaling requires the *Drosophila* Casein kinase 1ε encoded by *discs overgrown* (Dco), and we characterize candidate Dco phosphorylation sites in the Fat intracellular domain (ICD), the mutation of which impairs Fat-Hippo signaling. Through characterization of Dachs localization and directed membrane targeting of Dachs, we show that localization of Dachs influences both the Hippo and PCP pathways. Our results identify a conservation of Fat-PCP signaling mechanisms, establish distinct functions for different regions of the Fat ICD, support the correlation of Fat ICD phosphorylation with Fat-Hippo signaling, and confirm the importance of Dachs membrane localization to downstream signaling pathways.

KEY WORDS: Dachsous, *Drosophila*, Fat, Hippo, PCP, Polarity

INTRODUCTION

Organ morphogenesis requires coordination of growth with patterning processes that orient cell behaviors. The *Drosophila fat* gene encodes an atypical cadherin that functions as a receptor for signal transduction pathways that regulate growth (Hippo signaling) and planar cell polarity (PCP) (reviewed by Thomas and Strutt, 2012; Staley and Irvine, 2012). Fat is regulated by two proteins expressed in gradients: Dachsous (Ds) and Four-jointed (Fj). Ds encodes an atypical cadherin that can function as a ligand for Fat (reviewed by Thomas and Strutt, 2012; Staley and Irvine, 2012). Fj is a Golgi-localized kinase that phosphorylates cadherin domains of Fat and Ds to modulate binding between them (Ishikawa et al., 2008; Brittle et al., 2010; Simon et al., 2010). Rather than responding solely to the level of Ds and Fj, Fat is also regulated by the slope and vector of their expression gradients, with the slope influencing Hippo signaling and the vector influencing PCP (Rogulja et al., 2008; Willecke et al., 2008; Thomas and Strutt, 2012).

Fat is one of several upstream pathways that impinge on Hippo signaling (reviewed by Pan, 2010; Halder and Johnson, 2011; Staley and Irvine, 2012). Most of these upstream inputs converge on the kinase Warts (Wts), which negatively regulates the transcriptional co-activator Yorkie (Yki). Hippo pathway activity promotes Wts activity, which promotes cytoplasmic localization of Yki. When *fat*, *wts* or other upstream tumor suppressors are downregulated, then Yki accumulates in the nucleus, increasing the transcription of genes that promote growth. Three genes have been identified as playing key roles in Fat-Hippo signal transduction: *discs overgrown* (*dco*), *dachs* and *Zyxin* (*Zyx*). Dco is *Drosophila* Casein kinase 1ε (Zilian et al., 1999). An antimorphic allele, dco^3, specifically impairs Fat-Hippo signaling (Cho et al., 2006; Feng and Irvine, 2009). A portion of Fat is phosphorylated on its intracellular domain (ICD); this phosphorylation depends upon both Ds and Dco, suggesting that Fat ICD phosphorylation is a key step in Fat-Hippo signal transduction (Feng and Irvine, 2009; Sopko et al., 2009). Dachs is a myosin that downregulates Wts, and is required for the influence of *fat* or *dco* mutations on Hippo signaling (Cho and Irvine, 2004; Cho et al., 2006). Dachs localization is normally polarized in response to the Ds and Fj gradients (Mao et al., 2006; Rogulja et al., 2008; Ambegaonkar et al., 2012; Bosveld et al., 2012; Brittle et al., 2012). When Fat is overexpressed, Dachs membrane localization is reduced, whereas when *fat* is mutant, Dachs localizes to the membrane around the entire circumference of the cell (Mao et al., 2006). The correlation between Dachs localization and Fat activity suggests that regulation of Dachs localization is a key step in Fat signal transduction. Zyx affects Fat-Hippo signaling similarly to Dachs (Rauskolb et al., 2011). Zyx and Dachs can bind to each other, and binding of Dachs to Zyx stimulates Zyx-Wts binding (Rauskolb et al., 2011).

Dachs participates in both Fat-Hippo and Fat-PCP pathways, but it has been proposed that the influence of Dachs on Fat-Hippo signaling is related to the amount of Dachs localized to the membrane, whereas its influence on PCP is related to the direction in which Dachs membrane localization is polarized (Reddy and Irvine, 2008; Rogulja et al., 2008). One manifestation of Fat-PCP in the wing is the orientation of cell divisions, which contributes to wing elongation. In *fat*, *ds* or *dachs* mutants, cell division orientation is randomized, resulting in rounder wings (Baena-Lopez et al., 2008; Mao et al., 2011a). It has been proposed that Dachs myosin motor activity may contribute to the orientation of wing cell division by contracting cell apices, thereby altering cell geometry (Mao et al., 2011a). Modulation of tension along intercellular junctions also appears to contribute to influences of

Howard Hughes Medical Institute, Waksman Institute and Department of Molecular Biology and Biochemistry, Rutgers The State University of New Jersey, Piscataway, NJ 08854, USA.

*Present address: Memorial Sloan-Kettering Institute, 408 E 69th Street, New York, NY 10021, USA
‡Author for correspondence (irvine@waksman.rutgers.edu)

Accepted 3 December 2012

Dachs on PCP in the notum (Bosveld et al., 2012). A transcriptional co-repressor, Atrophin, has also been linked to some Fat-PCP phenotypes (Fanto et al., 2003; Li et al., 2009).

The central core of the Hippo pathway is conserved between *Drosophila* and mammals, but there is variation among upstream regulators (Pan, 2010; Halder and Johnson, 2011). Vertebrates have homologs of Fat (Fat4) and Ds (Dchs1), and depletion of Fat4 has been shown to affect Yap activity in a subset of CNS neurons in chick (Van Hateren et al., 2011). However, gene-targeted mutations in *Dchs1* or *Fat4* do not result in evident Hippo pathway phenotypes in mice, although they are consistent with influences of *Dchs1* and *Fat4* on PCP (Saburi et al., 2008; Mao et al., 2011b). Mammals do not, however, have an obvious Dachs homolog, and it remains unclear whether Fat signaling pathways in flies and mammals are related.

Here, we employ a structure-function approach to investigate signal transduction downstream of Fat. We show that Hippo and PCP pathways can be separated at the level of the Fat receptor. We identify point mutations in the Fat ICD that specifically impair Fat-Hippo signaling and reduce Fat phosphorylation, and identify a conserved four amino acid motif that is crucial for the effects of Fat on PCP. We also explore the relationship between Fat signaling and Dachs localization and provide direct evidence that Dachs localization influences both Hippo and PCP phenotypes.

MATERIALS AND METHODS

Drosophila genetics

Rescuing activity of Fat transgenes was characterized by crossing *fat^{GrV}/CyO,GFP; P[acman]-ft*/TM6b* or *ft^{8}/CyO,GFP; P[acman]-ft*/TM6b* to *ft^{Grv}/CyO.GFP*, *ft^{8}/CyOActGFP* or *ft^{GrV}/CyO,GFP; P[acman]-ft*/TM6b*, where *P[acman]-ft** indicates wild-type or mutant forms of *fat* rescue constructs. To overexpress Wts, *ft^{8} UAS-myc:Wts/CyOGFP* and *tub-$Gal4^{[LL7]}$* chromosomes were used. Clones expressing Dachs:Cit were made by crossing *hs-FLP; ft^{GrV}/CyO,GFP; P[acman]-ft*/TM6b* to *ft^{8}/CyO,GFP;act>CD2,y^{+}>dachs:cit/TM6b*.

To quantify wing area, male wings were traced using ImageJ (NIH) and areas were normalized to the average in controls. To quantify cross-vein distance, the length of vein L4 between cross-veins was measured using ImageJ and divided by the length of vein L3 to obtain a relative length, and these were normalized to the wild-type ratio. For mutant wings with incomplete cross-veins, points of crossing were estimated where possible based on the direction of the incomplete cross-vein. Hair polarity phenotypes were evaluated by the angle of deviation from the normal axis, and categorized as <30°, 30°-90° or >90° if more than 10% of wing hairs showed a deviation. Only the regions anterior to L3 and proximal to the posterior cross-vein were scored; costa and abdomens were scored independently using similar criteria.

Plasmids and constructs

Following recombineering techniques, the *Drosophila fat* ICD in the genomic construct was replaced by *galactose kinase* (*galK*) via positive selection, and then the *galK* was recombined with PCR fragments of *Fat4* ICDs by negative selection (Warming et al., 2005) (supplementary material Table S2). Recombineering was similarly used to introduce deletion or substitution mutations. Constructs were amplified by copy induction to enhance DNA yield (Venken et al., 2006) and supercoiled DNA was then purified and inserted into attP2 on 3L (Groth et al., 2004).

Histology and imaging

Imaginal discs were fixed and stained as described previously (Cho and Irvine, 2004) using mouse anti-Wg [1:800; 4D4, Developmental Studies Hybridoma Bank (DSHB)], rat anti-DE-Cadherin (1:40; DCAD2, DSHB), mouse anti-FLAG M2 (1:400; Sigma), mouse anti-V5 (1:400, preabsorbed; Invitrogen) and rat anti-Fat (1:1600). Fluorescent stains were captured on a Leica TCS SP5 confocal microscope. For horizontal sections, maximum projection through multiple sections was employed to allow visualization of staining in different focal planes. For protein polarization assessments, rose plots were generated using OSXStereonet (N. Cardoza, University of Stavanger).

Co-immunoprecipitation and western blotting

Co-immunoprecipitation from S2 cells was performed as described previously (Rauskolb et al., 2011) using anti-FLAG M2 beads (Sigma). For anti-Fat western blots, third instar wing discs were lysed in SDS-PAGE loading buffer supplemented with Protease Inhibitor Cocktail (Roche) and Phosphatase Inhibitor Cocktail Set II (Calbiochem) and stored at −80°C. Approximately 10-14 discs were loaded per lane, and the total protein amount was adjusted by normalizing to GAPDH. Primary antibodies used for blotting include rat anti-Fat (1:2000), mouse anti-GAPDH (1:10,000), rabbit anti-V5 (1:5000; Bethyl), rabbit anti-Wts (1:5000) and mouse anti-FLAG M2-HRP (1:10,000; Sigma). Detection was performed on a Li-Cor Odyssey imaging system, using goat anti-mouse IRdye680 and anti-rabbit IRdye800 (1:10,000; Li-Cor).

RESULTS

To elucidate Fat signal transduction mechanisms, we employed site-specific mutagenesis and phenotypic characterization. These experiments took advantage of the observation that *fat* null mutants can be rescued by genomic Bac clones containing a 39 kb region that includes the *fat* locus (Feng and Irvine, 2009). Despite the difficulty of manipulating these large genomic clones, we favored this approach over the expression of cDNAs under heterologous promoters because overexpression of Fat could obscure or bypass requirements for sequences that are normally essential for Fat activity.

Conservation of Fat-PCP signaling by mammalian Fat4

Functionally important sequence motifs can often be identified by evolutionary conservation. Mammals have four Fat genes, which share a similar extracellular domain (ECD) structure with *Drosophila* Fat and Kugelei (also known as Fat-like or Fat2) (Tanoue and Takeichi, 2005). Within the ICD, only Fat4 exhibits significant similarity to *Drosophila* Fat (Tanoue and Takeichi, 2005) (supplementary material Fig. S1). To assess the functional significance of this similarity, we investigated whether human FAT4 could rescue *Drosophila fat* mutants. As our goal was to investigate signal transduction by the ICD, we excluded potential differences between the ECDs by creating a hybrid transgene encoding the ECD of *Drosophila* Fat and the ICD of human FAT4 (Fat:Fat4) (supplementary material Fig. S2A,B). This was constructed within a *fat* genomic rescue construct (Feng and Irvine, 2009) by recombineering, and inserted using ΦC31-mediated site-specific recombination into the same location as we had previously inserted *Drosophila fat* (attP2 at 68A4) (Groth et al., 2004; Venken et al., 2006).

This Fat:Fat4 transgene could not rescue the lethality of *Drosophila fat* mutants. Moreover, examination of wing imaginal discs from *fat* mutant larvae expressing Fat:Fat4 revealed that they have the overgrown imaginal discs typical of *fat* mutants (supplementary material Fig. S2F), which indicates that they lack *Drosophila* Fat-Hippo signaling. In order to assess Fat-PCP signaling, we took advantage of the observation that the lethality and overgrowth phenotypes of *fat* mutations are suppressed by overexpressing Wts, whereas these flies still exhibit PCP phenotypes (Fig. 1A,E,H) (Feng and Irvine, 2007). Wing hairs normally point distally, but when *fat* activity is impaired wing hairs are misoriented and swirling patterns can be observed in the proximal wing. To quantify the effects on hair polarity, we

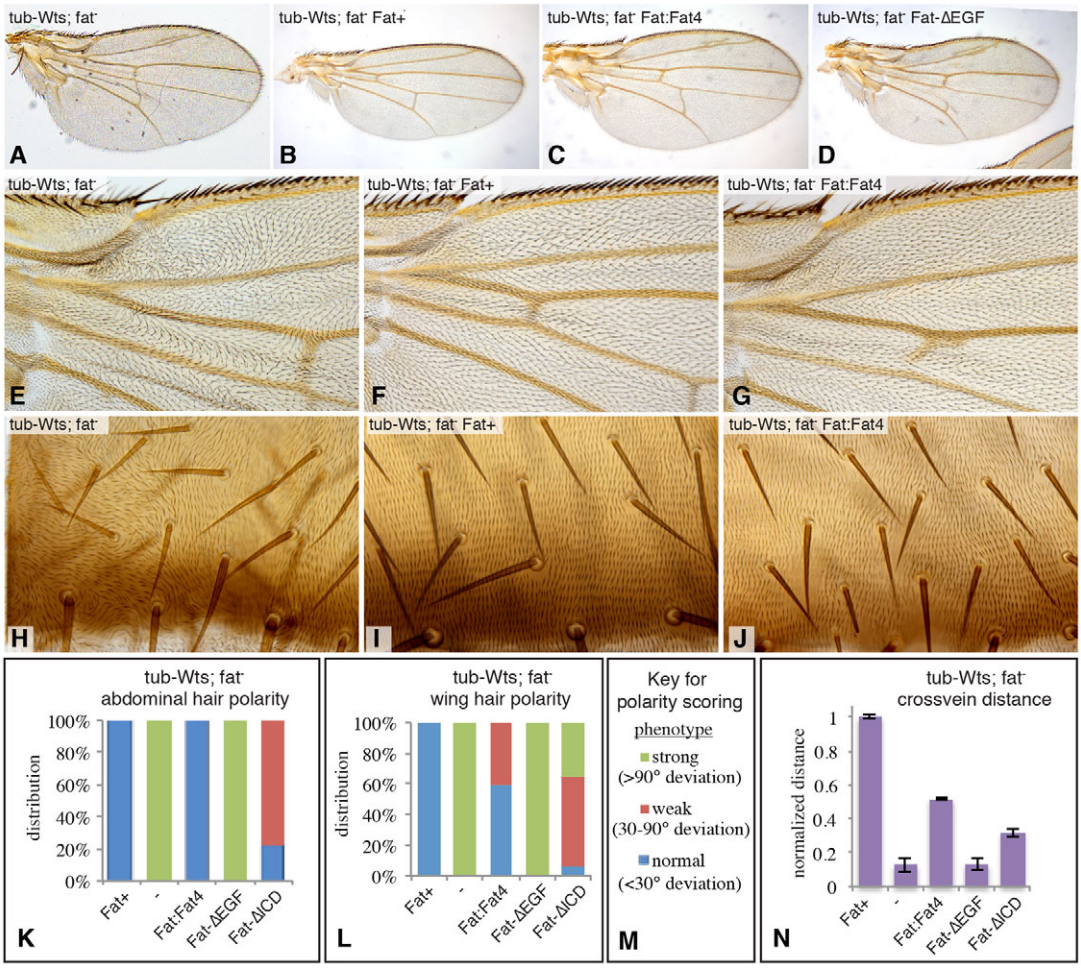

Fig. 1. Rescue of *fat* PCP phenotypes by FAT4. (**A-D**) Adult wings from $fat^{8}/fat^{G\text{-}rv}$ flies expressing (A) *tub-Gal4 UAS-wts* and (B) Fat^{+}, (C) *Fat:Fat4* or (D) *FatΔEGF.* (**E-G**) Proximal anterior wings from $fat^{8}/fat^{G\text{-}rv}$ flies expressing (E) *tub-Gal4 UAS-wts* and (F) Fat^{+}or (G) *Fat:Fat4.* (**H-J**) Abdominal segment from $fat^{8}/fat^{G\text{-}rv}$ flies expressing (H) *tub-Gal4 UAS-wts* and (I) Fat^{+} or (J) *Fat:Fat4.* (**K-M**) The distribution of PCP phenotypes (M) in abdomen (K) and proximal wing (L) for animals of the indicated genotypes. (**N**) Average distance between cross-veins in animals of the indicated genotypes, normalized to the value in wild-type-rescued animals. Error bars show s.e.m. Abbreviations for Fat transgenes are described in supplementary material Table S3.

classified wing hair PCP phenotypes as 'normal' when hair orientation was within 30° of its normal distal orientation, 'weak' when clusters of hairs (constituting >10% of hairs in the region examined) deviated in orientation by more than 30° but less than 90° from normal, and 'strong' when clusters of hairs deviated more than 90° from the normal orientation (Fig. 1M).

By these criteria, 100% of *fat* mutant wings rescued by a wild-type Fat transgene have a normal PCP phenotype, whereas 100% of Wts-rescued *fat* mutant wings have a strong PCP phenotype in the proximal, anterior wing (Fig. 1E,F,L). Using the same criteria, all *fat* mutant abdomens rescued by a wild-type Fat transgene have normal hair polarity, whereas all Wts-rescued *fat* mutant abdomens have a strong PCP phenotype (Fig. 1H,I,K). In *fat* mutants expressing Fat:Fat4 and Wts, PCP hair phenotypes were substantially rescued in the wing compared with Wts-expressing *fat* mutants without Fat transgenes, and were completely rescued in the abdomen (Fig. 1G,J-L). Fat:Fat4 also partially rescued the reduced cross-vein spacing phenotypes of *fat* mutants (Fig. 1C,N). Reduction of the distance between the anterior and posterior cross-veins is a classic Fat pathway mutant phenotype (Fig. 1A), which we think reflects the influence of Fat-PCP signaling on wing elongation. Wing elongation is influenced by Fat-PCP signaling both during disc growth, when it polarizes cell divisions along the proximal-distal axis, and during pupal development, when it influences local cell rearrangements (Baena-López et al., 2005; Aigouy et al., 2010; Mao et al., 2011a). This partial rescue of *fat* PCP phenotypes by Fat:Fat4 implies that mechanisms involved in Fat-PCP signal transduction are conserved from *Drosophila* to humans, and that they rely on shared structural motifs.

Identification of motifs required for distinct Fat signaling pathways

The overall sequence identity between the *Drosophila* Fat and human FAT4 ICDs is less than 25%, and most of this similarity is contained within six clusters of sequence identity (annotated A through F, Fig. 2; supplementary material Fig. S1). The functional significance of these regions of similarity was evaluated by deleting them within the *Drosophila* Bac clone that encompasses the *fat* locus. We also constructed one ECD mutation (FatΔEGF), in which four EGF domains, the significance of which have not been examined, were removed (supplementary material Fig. S2B).

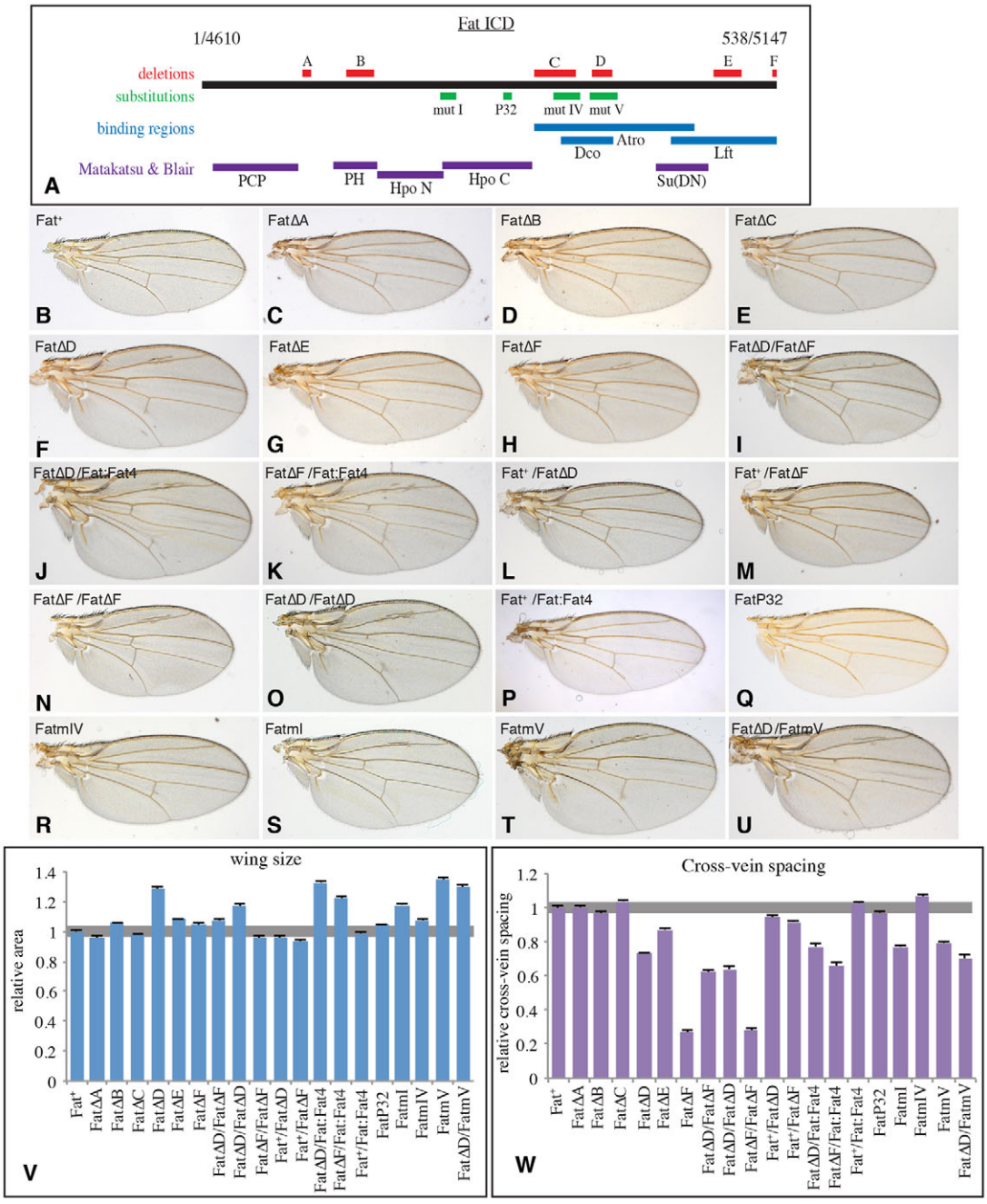

Fig. 2. Wing phenotypes associated with Fat intracellular domain motif mutations. (**A**) The Fat intracellular domain (ICD) showing the locations of mutations examined here (red and green bars), regions that bind Fat-associated proteins (blue bars), and functional regions identified by Matakatsu and Blair (Matakatsu and Blair, 2012) (purple). (**B-U**) Adult wings from $fat^{8}/fat^{G\text{-}rv}$ flies expressing (B) *Fat*$^{+}$, (C) *FatΔA*, (D) *FatΔB*, (E) *FatΔC*, (F) *FatΔD*, (G) *FatΔE*, (H) *FatΔF*, (I) *FatΔD/FatΔF*, (J) *FatΔD/Fat:Fat4*, (K) *FatΔF/Fat:Fat4*, (L) *Fat*$^{+}$*/FatΔD*, (M) *Fat*$^{+}$*/FatΔF*, (N) *FatΔF/FatΔF*, (O) *FatΔD/FatΔD*, (P) *Fat*$^{+}$*/Fat:Fat4*, (Q) *FatP32*, (R) *FatmIV*, (S) *FatmI*, (T) *FatmV*, (U) *FatΔD/FatmV.* (**V**) Average wing size in animals of the indicated genotypes, normalized to the value in wild-type-rescued animals. (**W**) Average distance between cross-veins in animals of the indicated genotypes, normalized to the value in wild-type-rescued animals. Additional statistics on wing measurements are in supplementary material Table S1. Error bars show s.e.m.

Transformed flies containing *fat* genomic rescue constructs with each of these seven mutations were obtained. None exhibited any dominant phenotypes. When they were crossed into *fat* mutant backgrounds, all six of the ICD deletions, but not FatΔEGF, rescued lethality (Fig. 2). Animals rescued by three of the ICD deletions (FatΔA, FatΔB and FatΔC) appeared morphologically normal (Fig. 2C-E; supplementary material Fig. S3), which implies that, despite their evolutionary conservation, these motifs are not essential. Conversely, animals rescued by constructs containing the other three deletions exhibited phenotypes that indicate that they provide only partial Fat activity.

In assays of wing growth, FatΔD-rescued *fat* mutants had wings that were obviously larger (by 29%) than normal, indicating a deficit in Fat-Hippo pathway activity (Fig. 2F,V). FatΔE-rescued

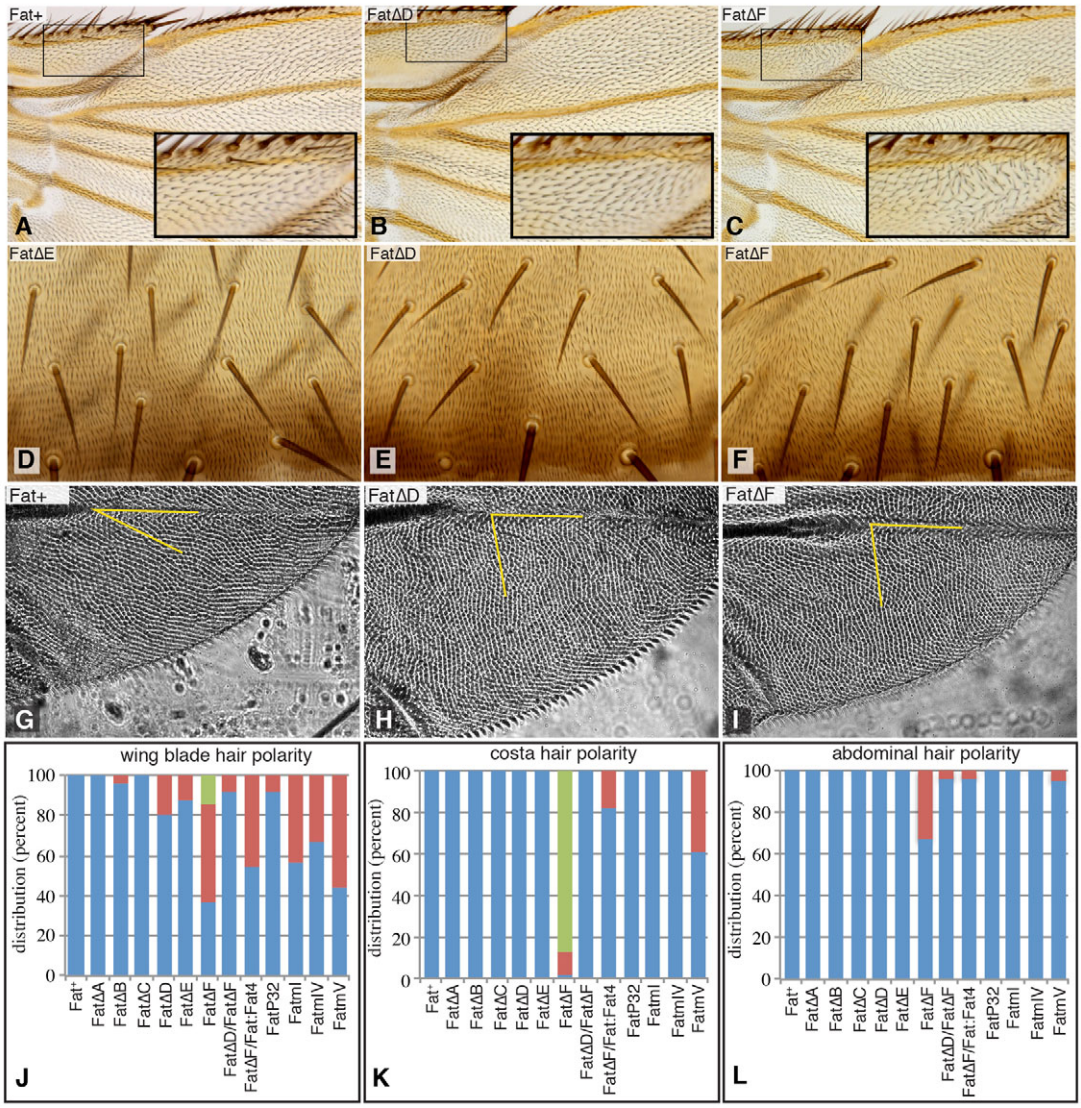

Fig. 3. PCP phenotypes associated with Fat ICD motif mutations. (**A-C**) Proximal anterior wings from $fat^{8}/fat^{G\text{-}rv}$ flies expressing (A) Fat^{+}, (B) *FatΔD* or (C) *FatΔF*. The boxed regions (costa) are magnified in the insets. (**D-F**) Abdomens from $fat^{8}/fat^{G\text{-}rv}$ flies expressing (D) *FatΔE*, (E) *FatΔD* or (F) *FatΔF*. (**G-I**) Proximal anterior wings, visualized by cuticle refraction microscopy (Doyle et al., 2008), from $fat^{8}/fat^{G\text{-}rv}$ flies expressing (G) Fat^{+}, (H) *FatΔD* or (I) *FatΔF*. Yellow lines indicate the estimated angle of ridges relative to the L4 vein. (**J-L**) The distribution of PCP phenotypes (see Fig. 1M) in (J) proximal wing, (K) costa and (L) abdomen for animals of the indicated genotypes.

fat mutant wings, by contrast, were on average only 8% larger than controls, a subtle, but nonetheless statistically significant difference (Fig. 2G,V; supplementary material Table S1). FatΔF-rescued *fat* mutant wings were only 4% larger than controls, which implies that Fat-Hippo signaling was almost fully rescued (Fig. 2H,V).

Although the area of FatΔF-rescued *fat* mutant wings was similar to that of wild type, they were shorter and wider than normal wings (Fig. 2H; supplementary material Table S1), which is suggestive of a PCP defect as the shape of the wing is influenced by oriented cell divisions and rearrangements. A PCP defect in FatΔF-rescued *fat* mutant wings was also implied by the short distance between cross-veins, which was only 27% of the wild-type distance (Fig. 2H,W). FatΔD and FatΔE mutants, by contrast, were more effective at rescuing cross-vein spacing, at 73% and 87% of the wild-type distance, respectively (Fig. 2F,G,W). *fat* wings rescued by FatΔA, FatΔB, FatΔC, FatΔD or FatΔE have negligible wing hair PCP phenotypes, indicating virtually complete rescue (Fig. 3; supplementary material Fig. S3). FatΔF-rescued wings, by contrast, exhibit hair PCP phenotypes. As the most proximal part of the anterior wing, the costa, was affected more severely than the wing blade, we scored these regions separately. Within the costa, most FatΔF-rescued wings exhibit a strong PCP phenotype, whereas in the rest of the wing the phenotype is mild (Fig. 3C,J,K). In the abdomen, a subtle phenotype was observed for FatΔF, whereas other transgenes fully rescued abdominal hair polarity (Fig. 3D-F,L; supplementary material Fig. S3).

We also analyzed the organization of intercellular ridges within the wing, the formation of which reflects polarized cellular organization (Doyle et al., 2008). Like wing hairs, ridges are influenced by both Frizzled and Fat-PCP pathways; however, ridge orientation is regulated separately from hair polarity (Hogan et al., 2011). In wild type, wing ridges run along the proximal-distal axis in the posterior wing, but along the anterior-posterior axis in the anterior wing (Fig. 3G; supplementary material Fig. S4) (Doyle et

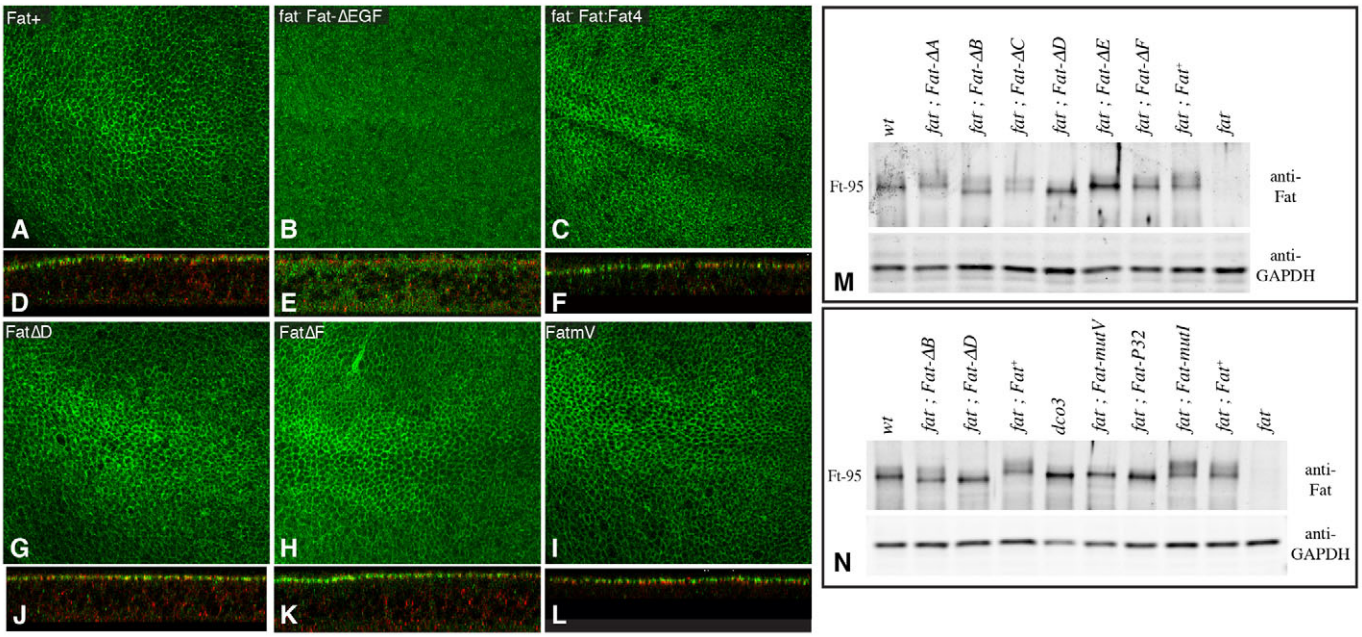

Fig. 4. Influence of *fat* mutations on Fat protein localization and mobility. (**A-L**) Confocal micrographs of Fat protein staining (green) in wing discs from $fat^{8}/fat^{G\text{-}rv}$ flies expressing (A,D) *P[acman]V5:fat[68A4]*, (B,E) *P[acman]V5:fatΔEGF[68A4]*, (C,F) *P[acman]V5:fat:FAT4[68A4]*, (G,J) *P[acman]V5:fatΔD[68A4]*, (H,K) *P[acman]V5:fatΔF[68A4]* or (I,L) *P[acman]V5:fat-mV[68A4].* Upper panels show horizontal sections, lower panels show vertical sections, with E-cadherin staining (red). (**M**,**N**) Western blots on wing disc lysates from animals of the indicated genotypes. Upper panel shows Fat antibody staining, lower panel shows a loading control (GAPDH).

al., 2008). When Fat signaling is disrupted by viable mutations, or RNAi of *ds* or *fat*, or in Wts-rescued *fat* mutants, then ridge orientation in the posterior wing is altered such that they now run in an anterior-posterior direction (Hogan et al., 2011) (supplementary material Fig. S4). Expression of *fat* genomic constructs with ΔA, ΔB, ΔC or ΔE mutations rescued posterior ridge orientation back to its wild-type, proximal-distal orientation (supplementary material Fig. S4), whereas neither FatΔD nor FatΔF was able to rescue ridge orientation (Fig. 3H,I).

The observation that some altered Fat transgenes are preferentially deficient in a subset of Fat signaling activities while retaining relatively normal activity in others implies that Fat signals through distinct downstream pathways that diverge at the level of Fat itself. As a genetic test of this proposal, we performed complementation tests. The results of these experiments were consistent with the hypothesis of separable Fat activities. For example, FatΔF largely rescued the overgrowth phenotype of FatΔD (adult wings were 7% larger than wings rescued by wild-type transgenes; Fig. 2I,V), and FatΔD provided substantial rescue of the PCP phenotypes of FatΔF (cross-vein spacing was 62% of wild type, and hair polarity was rescued; Fig. 2I,W; Fig. 3J-L; supplementary material Fig. S3). Conversely, mutations that impair the same Fat activity are not expected to complement. Thus, Fat:Fat4 failed to rescue the overgrowth of FatΔD-expressing wings (33% larger than wild type; Fig. 2J,V), but did partially rescue the cross-vein spacing defect (66% of wild type; Fig. 2K,W) and hair polarity phenotypes (Fig. 3; supplementary material Fig. S3) of FatΔF.

Since FatΔEGF was unable to rescue the lethality of *fat* mutations, we overexpressed Wts to assess PCP phenotypes. However, no PCP activity of FatΔEGF was detected, as by all of the criteria described above Wts-rescued *fat* mutants expressing ΔEGF were indistinguishable from Wts-rescued *fat* mutants without any Fat transgene (Fig. 1D,K-N; supplementary material Fig. S2G, Fig. S3A,K, Fig. S4G).

It has been reported that some Fat-PCP activity could be provided by overexpression of a Fat construct lacking the ICD in *fat* mutants, but not in *ds fat* double mutants (Casal et al., 2006; Matakatsu and Blair, 2012), presumably owing to an ability of the ECD of Fat to interact with Ds, and an ability of Ds to influence PCP independently of the Fat ICD. To evaluate whether the Fat ECD could provide Fat activity under endogenous expression conditions, we created and characterized a Fat isoform missing the ICD within our genomic rescue construct (supplementary material Fig. S2B). FatΔICD failed to rescue the lethality of *fat* mutants, and these animals had overgrown imaginal discs, consistent with the expected lack of Fat-Hippo pathway activity. However, when this lethality was rescued by Wts overexpression, partial PCP activity was detected. Cross-vein spacing can only be roughly estimated when Fat-Hippo activity is severely compromised because the cross-veins are often incomplete. Nonetheless, FatΔICD appeared to increase cross-vein spacing (Fig. 1N; supplementary material Fig. S2H). FatΔICD also partially rescued abdominal and wing hair polarity (Fig. 1K,L; supplementary material Fig. S3B,L), providing more Fat-PCP activity than FatΔEGF but less than Fat:Fat4 or FatΔF.

The influence of deletion mutations on Fat protein levels, localization and phosphorylation

To investigate the molecular basis for effects on Fat activity, we examined the localization, levels and potential modifications of the Fat proteins encoded by these transgenes. Fat-ΔEGF, which had no detectable Fat activity in any assay, was expressed, but immunostaining revealed that it was mislocalized, as it was detected within the cytoplasm and failed to accumulate at the normal subapical membrane location of Fat proteins (Fig. 4B,E).

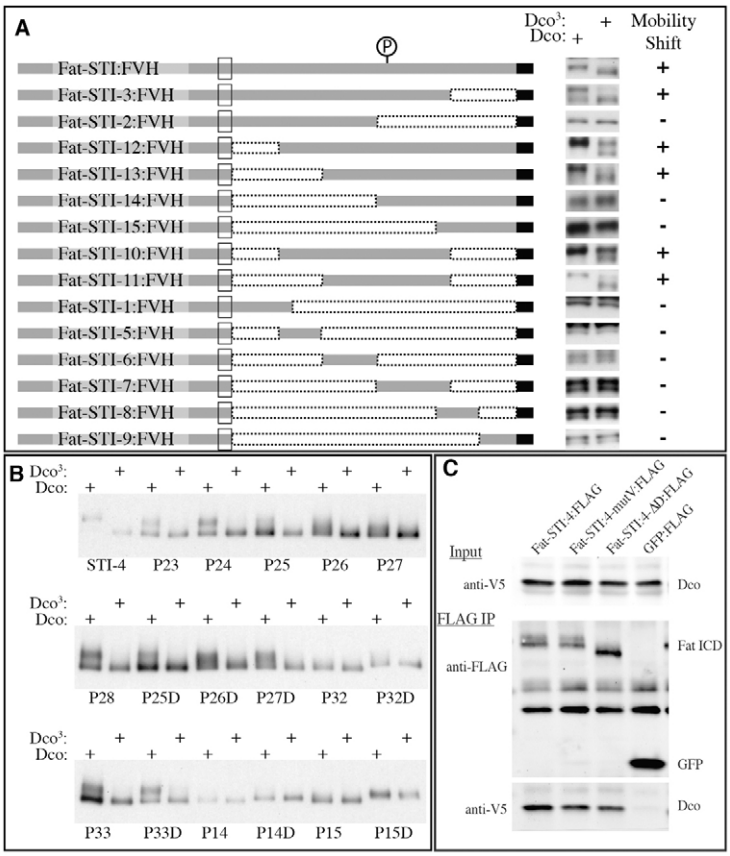

Fig. 5. Mapping Dco phosphorylation sites in Fat. (**A**) Deletion constructs used for mapping phosphorylation sites within the Fat ICD; truncations are indicated by dotted boxes, the open rectangle indicates the transmembrane domain and the black box indicates the epitope tags; P indicates the approximate position of the phosphorylation sites that influence Fat ICD mobility. To the right are shown portions of western blots of lysates of S2 cells expressing these constructs and Dco or Dco^3, with detectable mobility shift indicated by +. (**B**) Western blot on S2 cells expressing Fat-STI-4:FVH and point mutant derivatives, together with Dco or Dco^3, as indicated. The amino acids mutated are indicated in supplementary material Fig. S5; D indicates a Ser to Asp mutation; in other cases Ser to Ala mutations were employed. (**C**) Western blots showing results of co-immunoprecipitation experiments from lysates of S2 cells expressing Dco:V5 and the indicated FLAG-tagged Fat isoforms.

Thus, the complete lack of Fat activity associated with this transgene is likely to reflect misfolding and mislocalization. By contrast, all of the Fat transgenes that provided some Fat activity appeared to be expressed at normal levels and localized normally to the subapical membrane (Fig. 4; data not shown).

However, western blotting revealed an intriguing effect of the ΔD mutation on Fat protein mobility. In wild type, a fraction of Fat is phosphorylated on its ICD. This phosphorylation is visible as a mobility shift that results in the 95 kDa cleavage product appearing as a smeared doublet, with the reduced mobility of the upper band dependent upon phosphorylation (Feng and Irvine, 2009; Sopko et al., 2009). A similar smeared doublet was observed for all of the Fat deletion constructs that provide significant Fat-Hippo activity (ΔA, ΔB, ΔC, ΔE and ΔF) (Fig. 4M,N). For ΔD, by contrast, the relative fraction of the 95 kDa product that appeared in the upper band was reduced and the fraction in the lower band was increased, mimicking the influence of *dco*^{3} or *ds* mutations on Fat mobility (Feng and Irvine, 2009; Sopko et al., 2009) (Fig. 4M,N).

Identification of Dco phosphorylation sites

Independently of the analysis of conserved sequence motifs, the correlation between Fat phosphorylation and Fat-Hippo signaling led us to pursue the identification of Dco phosphorylation sites on Fat. As a similar Dco-dependent mobility shift of Fat is detected both *in vivo* and in cultured cells (Feng and Irvine, 2009; Sopko et al., 2009), we first used a cultured cell assay. The mobility of Fat constructs containing deletions of parts of the ICD was examined by western blotting lysates from cells co-expressing Dco or a mutant isoform that fails to phosphorylate Fat (Dco^3). A Fat polypeptide containing amino acids 172-415 of the ICD (ft-STI-11:FVH) was shifted by co-expression with Dco, whereas constructs encompassing further deletions of this region were not affected (Fig. 5A).

Since this suggested that either recognition by Dco, or the ability to detect a mobility shift, was lost when this region was further truncated, we turned to site-specific mutagenesis. Among a series of 20 constructs (P1 to P20) in which clusters of potential phosphorylation sites within this region were mutated (supplementary material Fig. S5), the mobility shift of 18 constructs appeared normal, whereas that of P14 and P15 was impaired (Fig. 5B; supplementary material Fig. S6). The ten Ser residues affected in P14 or P15 were then changed to Ala, alone and in combinations within 13 additional constructs (P21 to P33). This identified three Ser residues as contributing to the Dco-dependent mobility shift (Fig. 5B; supplementary material Fig. S6). When any of these Ser residues was individually mutated to Ala (P25, P26, P27), the mobility shift was reduced, and when all three were changed to Ala (P32) the mobility shift was eliminated (Fig. 5B). The introduction of a phosphomimetic residue, aspartic acid, into these sites (P15D, P32D) was sufficient to introduce a modest, Dco-independent, mobility shift (supplementary material Fig. S6B).

However, when the P15, P15D, P32 or P32D amino acid substitutions were engineered into *fat* genomic clones, the resulting transgenic flies all fully rescued *fat* mutants (Fig. 2Q,V; data not shown). Thus, these phosphorylation sites are not essential for Fat activity, even though the P32 mutation impaired the mobility shift of Ft-95 [the predominant C-terminal polypeptide produced by Fat processing (Feng and Irvine, 2009)] *in vivo* (Fig. 4N). To reconcile this with the evidence that Dco-dependent phosphorylation is linked to Fat activity, we hypothesized that there are multiple Dco sites on Fat, some of which visibly influence its mobility but are

not required for signal transduction, whereas others are required for signal transduction but do not affect mobility.

Thus, we made additional *fat* genomic constructs in which clusters of Ser and Thr residues were changed to Ala by mutagenesis and recombineering. Three constructs, each containing six to ten point mutations, were successfully created and transformed: Fat-mI, Fat-mIV and Fat-mV (supplementary material Figs S1, S5). Fat-mIV has virtually normal Fat activity, as rescued *fat* mutants did not appear significantly different from wild type (Figs 2, 3). By contrast, both Fat-mI and Fat-mV have only partial Fat activity, as rescued animals have overgrown wings (Fig. 2S,T,V). Fat-mV-rescued wings were similar in all respects to FatΔD-rescued wings (Figs 2, 3; supplementary material Figs S3, S4). Moreover, when the mobility of Fat-mV was examined, the slower migrating hyperphosphorylated form of Ft-95 was reduced compared with the faster migrating unphosphorylated form (Fig. 4N).

The region spanned by the point mutations in Fat-mV overlaps the region removed in Fat-ΔD (Fig. 2; supplementary material Fig. S1), and together they implicate this as a crucial region for the influence of Fat on Hippo signaling. They also both alter Fat mobility in a manner consistent with reduced phosphorylation of the Fat ICD (Fig. 4M,N), suggesting this as a region required for Fat phosphorylation *in vivo*. As this region overlaps a Dco binding site, we considered the possibility that they might reduce binding to Dco, thereby indirectly affecting other sites. However, introduction of the ΔD or mV mutations into a Fat ICD construct had no effect on its ability to bind Dco (Fig. 5C).

The increased wing size (18%) of Fat-mI-rescued animals was less than that for Fat-mV, and overall it exhibited only modest defects in PCP (Figs 2, 3; supplementary material Fig. S3). Nonetheless, the increased wing size implies that these point mutations impair Fat-Hippo signaling, and this region overlaps with a part of the Fat ICD identified by Matakatsu and Blair as important for Hippo signaling (Matakatsu and Blair, 2012). One curious feature of Fat-mI is that it actually appeared to increase Fat ICD phosphorylation, based on the mobility of Fat on SDS-PAGE gels (Fig. 4N).

Influence of *fat* mutations on Dachs localization

To investigate whether defects in Fat activity associated with ICD mutations correlate with effects on Dachs, we made clones of cells expressing a tagged Dachs isoform (Dachs:Cit) (Ambegaonkar et al., 2012) in *fat* mutants expressing *fat* genomic constructs representative of different phenotypic classes (FatΔD, FatΔF and Fat:Fat4) and compared them with *fat* mutants lacking a Fat transgene or expressing a wild-type Fat transgene.

Dachs:Cit localizes to the membrane around the entire circumference of the cell in *fat* mutant animals, whereas expression of wild-type V5:Fat rescues normal Dachs polarization (Fig. 6A,E). In both Fat:Fat4-rescued and FatΔD-rescued animals, an intermediate Dachs membrane localization phenotype was observed. Some clones of cells appeared to have increased Dachs membrane localization, and for some clones Dachs was detectable on the membrane completely surrounding the circumference of cells, as in *fat* mutants (Fig. 6B,D). By contrast, in other cases a polarized Dachs localization profile was detected. In FatΔF-rescued animals, a novel Dachs localization profile was observed, in which Dachs localization was usually polarized but the direction of polarization was variable (Fig. 6C).

To quantify these effects, Dachs localization images collected from *fat* mutants and from *fat* mutants rescued by Fat^{+}, Fat:Fat4, FatΔD or FatΔF transgenes were assigned random numbers and then scored together without knowledge of the genotypes. In this blind scoring, Dachs:Cit clones were first categorized as either non-polarized (Dachs localizes to the membrane around the circumference of the clone), multi-directional (Dachs localizes to the membrane around only part of a clone, but without a consistent direction of polarization), or unidirectional (Dachs is polarized in one direction). Then, among the unidirectional clones, the direction in which Dachs was polarized was scored. To simply this analysis, only clones in the medial two-thirds of the wing pouch were scored because in this region the distal polarization of Dachs points towards the dorsal-ventral compartment boundary, which can be identified by expression of Wg. In animals with Fat^{+} transgenes, 94% of clones were scored as unidirectional, and the vast majority of these were scored as having distally localized Dachs (Fig. 6F,G). Conversely, in *fat* mutant animals, only 13% of clones were scored as unidirectional, and of these few unidirectional clones only half were scored as having distally localized Dachs (Fig. 6F,K). Fat:Fat4-rescued and FatΔD-rescued animals were both intermediate in terms of the fraction of clones scored as non-polarized or unidirectional (Fig. 6F,H,J). FatΔF-rescued animals had a smaller fraction of non-polarized clones than Fat:Fat4 or FatΔD, and the largest fraction of multi-directional of all the genotypes (Fig. 6F). Moreover, among the unidirectional clones, the direction of polarization was partially randomized (Fig. 6I). These observations identify a correlation between the influence of Fat ICD mutations on Hippo or PCP signaling and their influence on Dachs localization.

Recent studies have revealed that Fat and Ds are themselves partially polarized in wing cells (Ambegaonkar et al., 2012; Brittle et al., 2012). To investigate whether the partial randomization of polarity in FatΔF occurs at the level of Fat localization, we took advantage of the observation that the polarized localization of Fat results in an anisotropy of Fat staining along proximal-distal interfaces as compared with anterior-posterior interfaces (Brittle et al., 2012). No difference in this anisotropy of localization was detected for a wild-type Fat construct versus FatΔF (Fig. 6L), which suggests that this mutation affects downstream signal transduction rather than Fat localization.

Influence of directed Dachs membrane localization on Hippo and PCP signaling

To confirm the importance of Dachs membrane localization and to distinguish it from other potential influences of Fat, we sought to localize Dachs to the membrane independently of *fat* mutation. One approach for membrane targeting is to attach a peptide sequence for lipidation. However, when a myristylation signal was attached to Dachs (Myr:Dachs), rather than activating Dachs it appeared to create a dominant-negative protein, as expression of Myr:Dachs phenocopied *dachs* mutations (Fig. 7E,P). Dachs normally exhibits very discrete localization at the subapical membrane, near E-cadherin, whereas Myr:Dachs is broadly localized on membranes throughout the cell (Fig. 7G,H). Thus, we sought an alternative approach that would target Dachs to the correct location.

Studies of Zyx have identified it as a component of the Fat-Hippo pathway and suggested a model in which Dachs acts at the membrane in association with Zyx (Rauskolb et al., 2011). Thus, we constructed a Zyx:Dachs fusion protein, expressed under UAS control. This fusion protein exhibited a Zyx-like

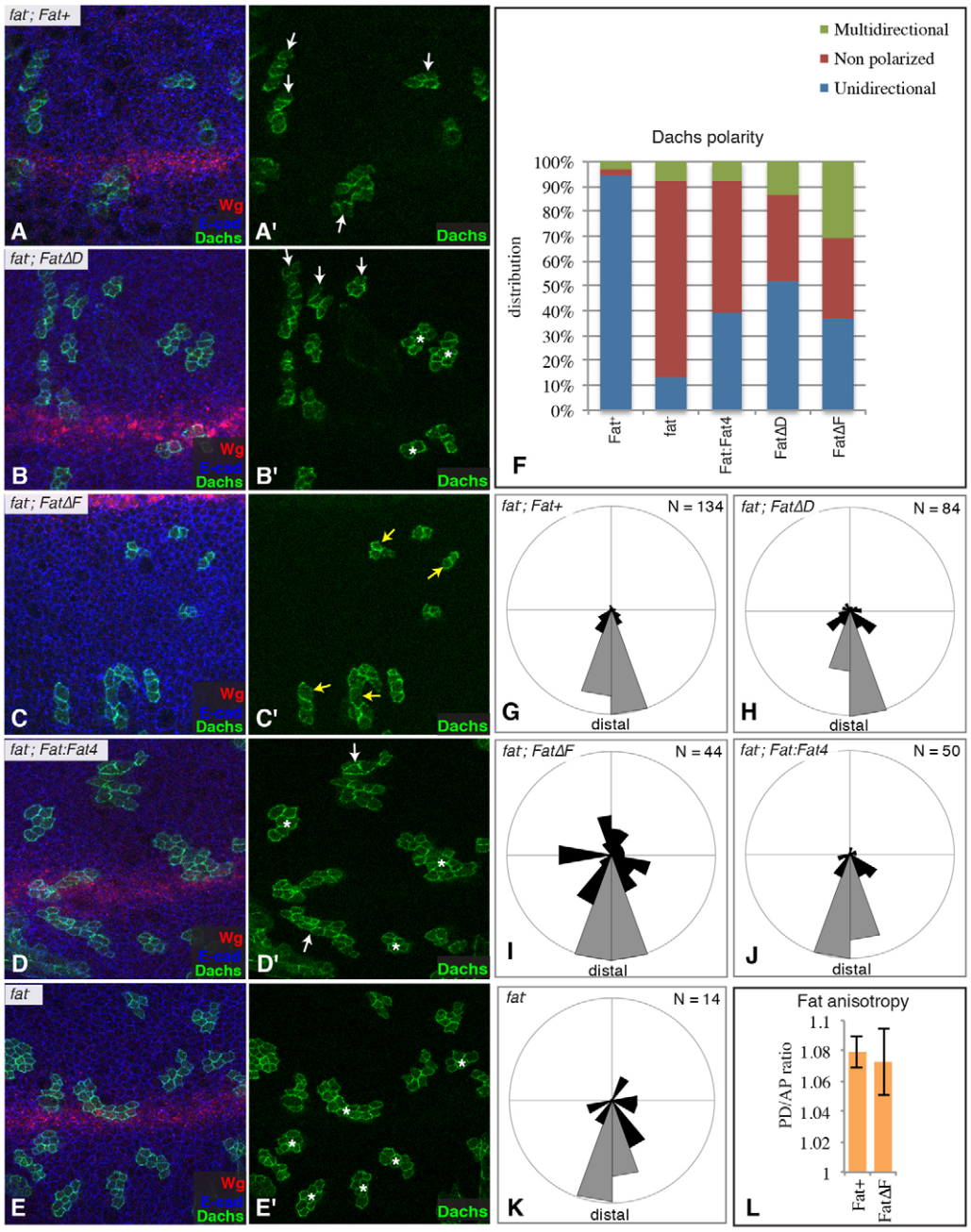

Fig. 6. Influence of targeted *fat* mutations on Dachs localization. (**A-E′**) Examples of wing discs from animals of the indicated genotypes, with clones of cells expressing Dachs:Cit (green) from an AyDachs:Cit transgene. These discs are stained for expression of Wg (red; marks dorsal-ventral boundary) and E-cad (blue; outlines cells). The polarity of Dachs localization is indicated by the arrows pointing in the direction of Dachs:Cit membrane localization; white arrows indicate normal polarity, yellow arrows abnormal polarity; asterisks indicate lack of polarity. (A′-E′) The Dachs:Cit channel only. (**F**) The distribution of Dachs polarization phenotypes in animals of the indicated genotypes. Distributions were scored blind and over 100 Dachs:Cit clones were scored per genotype. (**G-K**) Rose plots depicting the vectors of Dachs:Cit polarization identified within polarized clones in discs of animals of the indicated genotypes. Polarities were scored blind; the number scored is shown top left. The diagrams are oriented with proximal at the top, anterior right and distal at bottom (defined by Wg expression). Normal distal polarization is in gray. (**L**) Anisotropy of Fat staining along proximal-distal versus anterior-posterior interfaces. ImageJ was used to calculate average staining intensities along all cell interfaces within the central region of the wing pouch, from five to six different discs, that could be defined as predominantly proximal-distal or anterior-posterior based on comparison with Wg staining. Error bars indicate s.e.m.

localization profile, as it localized to the subapical membrane around the entire circumference of the cell, rather than exhibiting the polarized localization characteristic of Dachs (Fig. 7I,J). When expressed in the developing wing under *nub-Gal4* control, it resulted in a strong wing overgrowth phenotype (Fig. 7F), and, like reductions of *fat*, it decreased Wts levels (Fig. 7K). These overgrown wings did not flatten properly, and hence it was difficult to compare their size with wings co-expressing wild-

type forms of Zyx and Dachs, which also overgrow (Fig. 7D), but Zyx:Dachs-expressing wings nonetheless appeared to be slightly larger. A stronger activation of Yki was also evident when comparing wing discs expressing the Zyx:Dachs fusion protein with wing discs co-expressing Zyx and Dachs – the discs became more highly folded, which can be a consequence of overgrowth, and a Yki target gene, *ex-lacZ*, was highly expressed (Fig. 7Q). The consequences of fusing Zyx and Dachs was even more dramatic when PCP was examined, as co-overexpression of Zyx and Dachs does not have significant effects on hair polarity (Fig. 7S), whereas expression of Zyx:Dachs resulted in a strong disturbance of wing hair polarity (Fig. 7T). Thus, targeting Dachs to the membrane by fusing it with Zyx phenocopies both the Hippo and PCP phenotypes of *fat* mutants.

DISCUSSION

Distinct regions of Fat required for Hippo and PCP signaling

Our results indicate that the effects of Fat on wing growth versus PCP can be separated at the level of Fat itself: a four amino acid deletion at the C-terminus of Fat (FatΔF) impairs PCP but does not affect wing growth, whereas deletion or point mutations within the D motif (FatΔD, Fat-mV) result in wing overgrowth but have weaker effects than FatΔF on PCP. Matakatsu and Blair (Matakatsu and Blair, 2012) also recently reported that they could separate regions of Fat required for Hippo and PCP activities, but identified completely different regions.

Matakatsu and Blair used UAS-driven expression, whereas we used genomic constructs. Because these large constructs are more difficult to manipulate, we did not undertake a detailed analysis of the entire ICD, but focused on candidate regions. However, our approach had the advantage that expression under endogenous conditions could identify activities that are missed when proteins are overexpressed. Thus, we observed wing overgrowth when region D was mutated, but this region was not identified by Matakatsu and Blair. Nonetheless, the ΔD and mV mutations only partially impair Fat-Hippo activity, as they rescue the lethality of *fat* mutants, and additional Hippo activity is presumably provided by regions identified by Matakatsu and Blair (Matakatsu and Blair, 2012), which are not conserved in Fat4. Hence, our combined studies imply that multiple regions of the Fat ICD contribute to Fat-Hippo signaling.

PCP was first recognized for its effects on the orientation of hairs on the body of the fly, but is now understood to encompass a wider range of cellular polarization. Matakatsu and Blair only examined hair polarity in their assessments of PCP, whereas we also considered Dachs polarization, ridge orientation and cross-vein spacing (because cross-vein spacing is also reduced by Fat overexpression, it could not be assessed by their approach). Outside of the costa, deletion of the F region had only minor effects on hair polarity. Instead, the PCP phenotypes of FatΔF were most noticeable when cross-vein spacing, Dachs localization or ridge orientation was examined. Thus, the assignment of PCP activity to distinct regions of the Fat ICD by our studies does not represent a disagreement, but rather emphasizes that there are different types of PCP that can be genetically separated.

The ability to analyze PCP phenotypes for Fat constructs that do not rescue lethality depends upon Wts overexpression. The wing hair PCP phenotype of these animals is restricted to the proximal wing. Moreover, they have strong disruptions of abdominal PCP, but typically only part of each abdominal segment is affected. Indeed, the hair phenotype of Wts-rescued *fat* mutants appears to be similar to that described for *fat* mutants rescued by λfatICD, a construct that contains just the Fat ICD, which has been interpreted as a partial rescue of hair polarity (Matakatsu and Blair, 2012). We suggest, therefore, that some of the hair PCP phenotype ascribed to *fat* could reflect effects on transcription of downstream target genes, mediated via downregulation of Wts. Our results also support the conclusion that some of the influence of Fat on PCP reflects an activity of the ECD as a ligand for Ds, indicating that Ds-Fat-PCP signaling is bidirectional, with Fat and Ds acting as both receptor and ligand for each other. Previous experiments showed that, when overexpressed, the Fat ECD could influence PCP in a Ds-dependent fashion (Casal et al., 2006; Matakatsu and Blair, 2012); we have now confirmed that FatΔICD partially rescues *fat* PCP phenotypes even at endogenous expression levels.

A conserved motif required for Fat-PCP signaling

Fat4 and *Dchs1* mutant mice have phenotypes that are consistent with effects on PCP (Saburi et al., 2008; Mao et al., 2011b), but the molecular mechanisms involved are unknown. The ability of Fat:Fat4 to rescue *fat* PCP phenotypes indicates that there are conserved mechanisms of Fat-PCP signaling involving the Fat ICD. Among the conserved sequence motifs, the four amino acid F motif is clearly required for PCP, which implicates it as being involved in a conserved PCP mechanism. These four amino acids resemble a PDZ domain-binding motif, suggesting that it might interact with a PDZ domain-containing protein.

A striking feature of FatΔF-rescued *fat* mutants is the partial randomization of Dachs polarization. The observation that Dachs can be polarized, but in a variable direction, suggests that there are multiple steps involved in establishing Dachs polarization, i.e. control over whether Dachs localization is polarized can be mechanistically uncoupled from control over the direction in which Dachs is polarized.

Role of Dachs localization in Fat signaling

The observation of both randomized Dachs localization and rounder wings with more closely spaced cross-veins in FatΔF-rescued animals extends the correlation between polarized Dachs localization and PCP phenotypes, and is consistent with the hypothesis that Dachs polarization directs polarized cell behaviors. We also found a rough correlation between the decreased Fat-Hippo pathway activity of Fat:Fat4 or FatΔD and increased detection of Dachs at the subapical membrane. These results are at least generally consistent with the hypothesis that the direction in which Dachs localization is polarized influences PCP, whereas the amount of Dachs on the membrane influences Hippo signaling (Mao et al., 2006; Reddy and Irvine, 2008; Rogulja et al., 2008).

These and other studies have identified a correlation between Dachs localization and Fat signaling, but could not prove that altered Dachs localization is a cause rather than a consequence of Fat signal transduction, nor separate the role of Dachs localization from other potential effects of Fat. We have now directly confirmed the importance of Dachs localization by creating a Zyx:Dachs fusion protein, the expression of which in otherwise wild-type animals phenocopies *fat* mutants both for wing growth and PCP phenotypes.

Role of Fat phosphorylation in Fat-Hippo signaling

Despite our extensive investigation of potential phosphorylation sites, the role of Fat receptor phosphorylation in signal transduction remains elusive. Fat is directly phosphorylated by Dco, which is

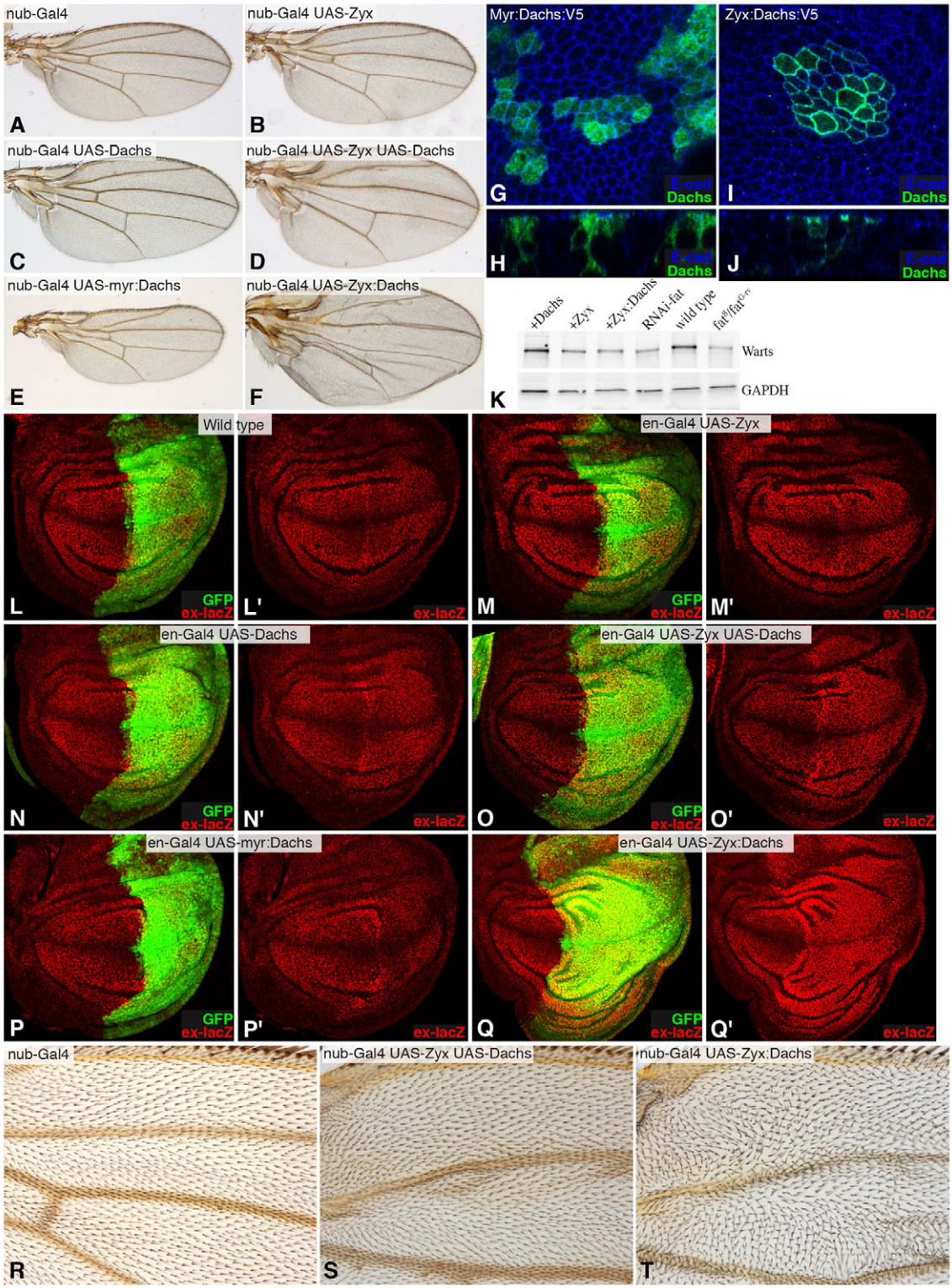

Fig. 7. Influence of membrane-tethered Dachs on wing growth and PCP. (**A-F**) Adult wings from animals expressing *nub-Gal4* and (B) *UAS-Zyx*, (C) *UAS-dachs*, (D) *UAS-Zyx UAS-dachs*, (E) *UAS-myr:dachs* or (F) *UAS-Zyx:dachs*. (**G-J**) Localization of membrane-tethered Dachs constructs, showing clones of cells expressing (G,H) Myr:Dachs:V5 (green) or (I,J) Zyx:Dachs:V5 (green) in (G,I) horizontal or (H,J) vertical section. (**K**) Western blot on lysates of wing discs expressing *tub-Gal4* and *UAS-dachs*, *UAS-Zyx*, *UAS-Zyx:dachs*, or *UAS-RNAi-fat*, or mutant for *fat*, as indicated. Loss of Fat activity reduces Wts protein levels (Cho et al., 2006). GAPDH serves as a loading control. Mean Wts levels from four independent experiments, normalized to Wts levels in *fat* mutants, were: *UAS-dachs* 3.3, *UAS-Zyx* 3.6, *UAS-Zyx:dachs* 3.3, *UAS-RNAi-fat* 1.8, wild type 5.0, and *fat* mutant 1.0. (**L-Q′**) Wing discs from animals expressing (L) *en-Gal4* (marked by *UAS-GFP*, green) and (M) *UAS-Zyx*, (N) *UAS-dachs*, (O) *UAS-Zyx UAS-dachs*, (P) *UAS-myr:dachs* or (Q) *UAS-Zyx:dachs*, stained for *ex-lacZ* (red). (L′-Q′) *ex-lacZ* channel only. (**R-T**) Anterior proximal wing from animals expressing (R) *nub-Gal4* and (S) *UAS-Zyx UAS-dachs* and (T) *UAS-Zyx:dachs*.

required for Fat-Hippo signaling, and acts genetically upstream of *dachs* and *Zyx* (Cho et al., 2006; Feng and Irvine, 2009; Sopko et al., 2009; Rauskolb et al., 2011). Moreover, Fat ICD phosphorylation correlates with Fat activity, as it is reduced in dco^3 or *ds* mutants, or when there are mutations in Fat that impair Fat-Hippo signaling (FatΔD, Fat-mV). However, other Fat ICD mutations impair Fat phosphorylation without affecting Fat signaling (Fat-P32, Fat-P15). Moreover, dco^3 does not affect Dachs localization, but FatΔD, which impairs Fat-Hippo signaling and Fat phosphorylation, does affect Dachs localization. To reconcile these observations, we propose that Dco normally blocks the ability of Zyx and Dachs to inactivate Wts through a mechanism that is independent of the influence of Fat on Dachs localization. Fat might be the key substrate of Dco in this process, but our results are equally consistent with the possibility that phosphorylation of the Fat ICD by Dco is a consequence, not a cause, of Fat receptor activation. Thus, although it can serve as a marker of Fat activity, the biologically important substrate of Dco might be some other protein.

Acknowledgements
We thank Binnaz Kucuk for creating Myr:Dachs; Tahia Haque for assisting in preliminary characterization of *fat* deletion constructs; and the DSHB and the Bloomington Stock Center for antibodies and *Drosophila* stocks.

Funding
This research was supported by the Howard Hughes Medical Institute and National Institutes of Health [grant 2R01GM078620]. Deposited in PMC for release after 6 months.

Competing interests statement
The authors declare no competing financial interests.

Supplementary material
Supplementary material available online at
http://dev.biologists.org/lookup/suppl/doi:10.1242/dev.088534/-/DC1

References

Aigouy, B., Farhadifar, R., Staple, D. B., Sagner, A., Röper, J.-C., Jülicher, F. and Eaton, S. (2010). Cell flow reorients the axis of planar polarity in the wing epithelium of Drosophila. *Cell* **142**, 773-786.
Ambegaonkar, A. A., Pan, G., Mani, M., Feng, Y. and Irvine, K. D. (2012). Propagation of Dachsous-Fat planar cell polarity. *Curr. Biol.* **22**, 1302-1308.
Baena-López, L. A., Baonza, A. and García-Bellido, A. (2005). The orientation of cell divisions determines the shape of Drosophila organs. *Curr. Biol.* **15**, 1640-1644.
Baena-Lopez, L. A., Rodríguez, I. and Baonza, A. (2008). The tumor suppressor genes dachsous and fat modulate different signalling pathways by regulating dally and dally-like. *Proc. Natl. Acad. Sci. USA* **105**, 9645-9650.
Bosveld, F., Bonnet, I., Guirao, B., Tlili, S., Wang, Z., Petitalot, A., Marchand, R., Bardet, P. L., Marcq, P., Graner, F. et al. (2012). Mechanical control of morphogenesis by Fat/Dachsous/Four-jointed planar cell polarity pathway. *Science* **336**, 724-727.
Brittle, A. L., Repiso, A., Casal, J., Lawrence, P. A. and Strutt, D. (2010). Four-jointed modulates growth and planar polarity by reducing the affinity of dachsous for fat. *Curr. Biol.* **20**, 803-810.
Brittle, A., Thomas, C. and Strutt, D. (2012). Planar polarity specification through asymmetric subcellular localization of Fat and Dachsous. *Curr. Biol.* **22**, 907-914.
Casal, J., Lawrence, P. A. and Struhl, G. (2006). Two separate molecular systems, Dachsous/Fat and Starry night/Frizzled, act independently to confer planar cell polarity. *Development* **133**, 4561-4572.
Cho, E. and Irvine, K. D. (2004). Action of fat, four-jointed, dachsous and dachs in distal-to-proximal wing signaling. *Development* **131**, 4489-4500.
Cho, E., Feng, Y., Rauskolb, C., Maitra, S., Fehon, R. and Irvine, K. D. (2006). Delineation of a Fat tumor suppressor pathway. *Nat. Genet.* **38**, 1142-1150.
Doyle, K., Hogan, J., Lester, M. and Collier, S. (2008). The Frizzled Planar Cell Polarity signaling pathway controls Drosophila wing topography. *Dev. Biol.* **317**, 354-367.
Fanto, M., Clayton, L., Meredith, J., Hardiman, K., Charroux, B., Kerridge, S. and McNeill, H. (2003). The tumor-suppressor and cell adhesion molecule Fat controls planar polarity via physical interactions with Atrophin, a transcriptional co-repressor. *Development* **130**, 763-774.
Feng, Y. and Irvine, K. D. (2007). Fat and expanded act in parallel to regulate growth through warts. *Proc. Natl. Acad. Sci. USA* **104**, 20362-20367.
Feng, Y. and Irvine, K. D. (2009). Processing and phosphorylation of the Fat receptor. *Proc. Natl. Acad. Sci. USA* **106**, 11989-11994.
Groth, A. C., Fish, M., Nusse, R. and Calos, M. P. (2004). Construction of transgenic Drosophila by using the site-specific integrase from phage phiC31. *Genetics* **166**, 1775-1782.
Halder, G. and Johnson, R. L. (2011). Hippo signaling: growth control and beyond. *Development* **138**, 9-22.
Hogan, J., Valentine, M., Cox, C., Doyle, K. and Collier, S. (2011). Two frizzled planar cell polarity signals in the Drosophila wing are differentially organized by the Fat/Dachsous pathway. *PLoS Genet.* **7**, e1001305.
Ishikawa, H. O., Takeuchi, H., Haltiwanger, R. S. and Irvine, K. D. (2008). Four-jointed is a Golgi kinase that phosphorylates a subset of cadherin domains. *Science* **321**, 401-404.
Li, W., Kale, A. and Baker, N. E. (2009). Oriented cell division as a response to cell death and cell competition. *Curr. Biol.* **19**, 1821-1826.
Mao, Y., Rauskolb, C., Cho, E., Hu, W. L., Hayter, H., Minihan, G., Katz, F. N. and Irvine, K. D. (2006). Dachs: an unconventional myosin that functions downstream of Fat to regulate growth, affinity and gene expression in Drosophila. *Development* **133**, 2539-2551.
Mao, Y., Tournier, A. L., Bates, P. A., Gale, J. E., Tapon, N. and Thompson, B. J. (2011a). Planar polarization of the atypical myosin Dachs orients cell divisions in Drosophila. *Genes Dev.* **25**, 131-136.
Mao, Y., Mulvaney, J., Zakaria, S., Yu, T., Morgan, K. M., Allen, S., Basson, M. A., Francis-West, P. and Irvine, K. D. (2011b). Characterization of a Dchs1 mutant mouse reveals requirements for Dchs1-Fat4 signaling during mammalian development. *Development* **138**, 947-957.
Matakatsu, H. and Blair, S. S. (2012). Separating planar cell polarity and Hippo pathway activities of the protocadherins Fat and Dachsous. *Development* **139**, 1498-1508.
Pan, D. (2010). The hippo signaling pathway in development and cancer. *Dev. Cell* **19**, 491-505.
Rauskolb, C., Pan, G., Reddy, B. V., Oh, H. and Irvine, K. D. (2011). Zyxin links fat signaling to the hippo pathway. *PLoS Biol.* **9**, e1000624.
Reddy, B. V. and Irvine, K. D. (2008). The Fat and Warts signaling pathways: new insights into their regulation, mechanism and conservation. *Development* **135**, 2827-2838.
Rogulja, D., Rauskolb, C. and Irvine, K. D. (2008). Morphogen control of wing growth through the Fat signaling pathway. *Dev. Cell* **15**, 309-321.
Saburi, S., Hester, I., Fischer, E., Pontoglio, M., Eremina, V., Gessler, M., Quaggin, S. E., Harrison, R., Mount, R. and McNeill, H. (2008). Loss of Fat4 disrupts PCP signaling and oriented cell division and leads to cystic kidney disease. *Nat. Genet.* **40**, 1010-1015.
Simon, M. A., Xu, A., Ishikawa, H. O. and Irvine, K. D. (2010). Modulation of fat:dachsous binding by the cadherin domain kinase four-jointed. *Curr. Biol.* **20**, 811-817.
Sopko, R., Silva, E., Clayton, L., Gardano, L., Barrios-Rodiles, M., Wrana, J., Varelas, X., Arbouzova, N. I., Shaw, S., Saburi, S. et al. (2009). Phosphorylation of the tumor suppressor fat is regulated by its ligand Dachsous and the kinase discs overgrown. *Curr. Biol.* **19**, 1112-1117.
Staley, B. K. and Irvine, K. D. (2012). Hippo signaling in Drosophila: recent advances and insights. *Dev. Dyn.* **241**, 3-15.
Tanoue, T. and Takeichi, M. (2005). New insights into Fat cadherins. *J. Cell Sci.* **118**, 2347-2353.
Thomas, C. and Strutt, D. (2012). The roles of the cadherins Fat and Dachsous in planar polarity specification in Drosophila. *Dev. Dyn.* **241**, 27-39.
Van Hateren, N. J., Das, R. M., Hautbergue, G. M., Borycki, A. G., Placzek, M. and Wilson, S. A. (2011). FatJ acts via the Hippo mediator Yap1 to restrict the size of neural progenitor cell pools. *Development* **138**, 1893-1902.
Venken, K. J., He, Y., Hoskins, R. A. and Bellen, H. J. (2006). P[acman]: a BAC transgenic platform for targeted insertion of large DNA fragments in D. melanogaster. *Science* **314**, 1747-1751.
Warming, S., Costantino, N., Court, D. L., Jenkins, N. A. and Copeland, N. G. (2005). Simple and highly efficient BAC recombineering using galK selection 10.1093/nar/gni035. *Nucleic Acids Res.* **33**, e36.
Willecke, M., Hamaratoglu, F., Sansores-Garcia, L., Tao, C. and Halder, G. (2008). Boundaries of Dachsous Cadherin activity modulate the Hippo signaling pathway to induce cell proliferation. *Proc. Natl. Acad. Sci. USA* **105**, 14897-14902.
Zilian, O., Frei, E., Burke, R., Brentrup, D., Gutjahr, T., Bryant, P. J. and Noll, M. (1999). double-time is identical to discs overgrown, which is required for cell survival, proliferation and growth arrest in Drosophila imaginal discs. *Development* **126**, 5409-5420.

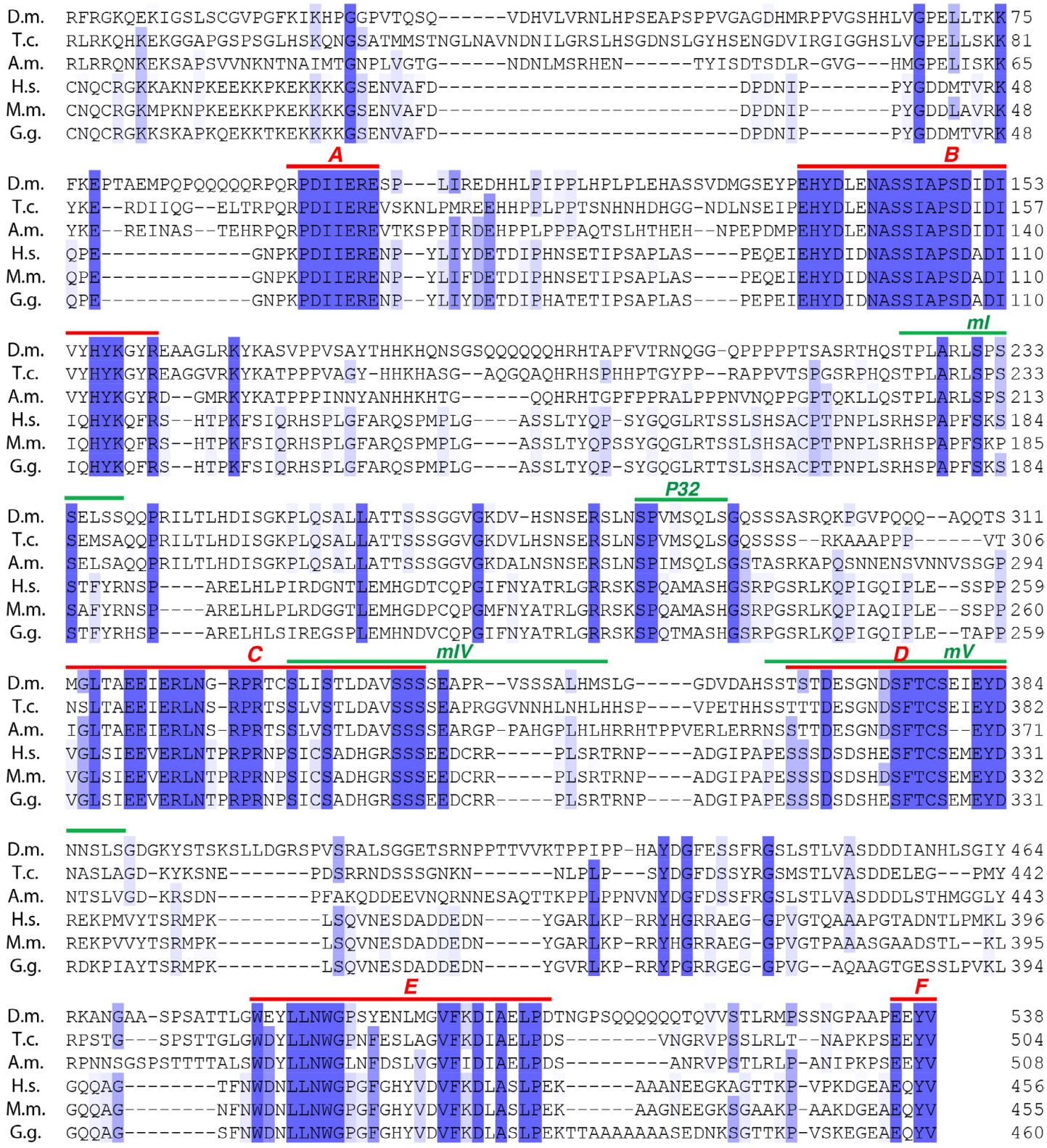

Fig. S1. Alignment of Fat ICD sequences. ClustalW alignment of intracellular domains (generated at the NCBI web site) of three insect Fat sequences (D.m., *Drosophila melanogaster*; T.c., *Tribolium castaneum*; A.m., *Apis mellifera*) and three vertebrate Fat4 sequences (H.s., *Homo sapiens*; M.m., *Mus musculus*; G.g., *Gallus gallus*). Based on transmembrane domain predictions, the ICD in *D. melanogaster* Fat is 538 amino acids, and begins at amino acid 4610. Sequence identity is indicated by relative shading. Conserved motifs deleted by mutations are indicated by red lines and regions affected by point mutations are indicated by green lines; the specific Ser and Thr residues changed in these point mutations are indicated in Fig. S5.

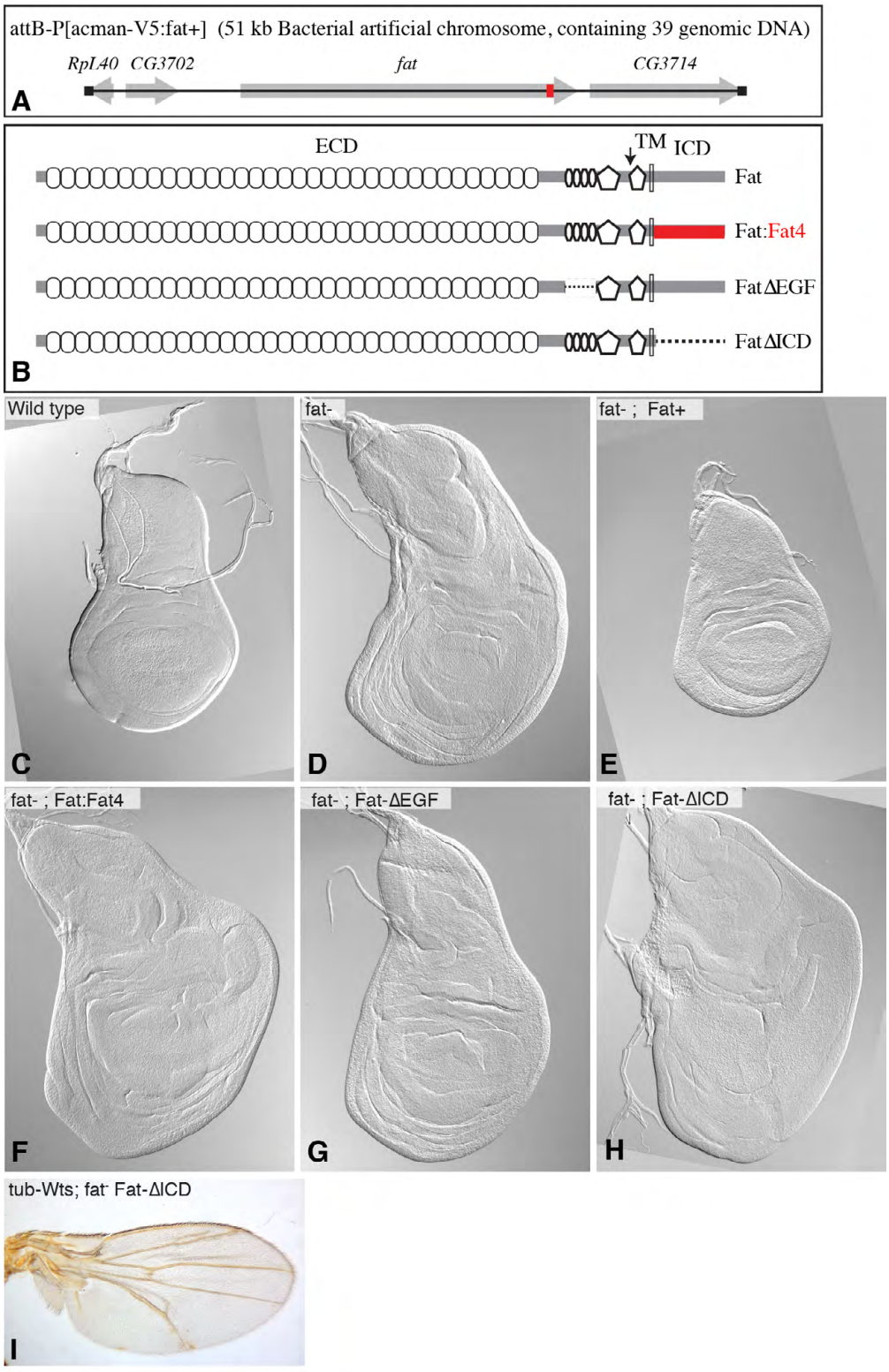

Fig. S2. Additional analysis of Fat constructs that fail to rescue *fat* mutant lethality. (**A**) The *fat* locus genomic rescue construct, with the region encoding the ICD highlighted in red. (**B**) Wild-type (top) and three mutant forms of Fat examined; red indicates replacement of the *Drosophila* ICD by the human FAT4 ICD. (**C-H**) Examples of wing discs from representative late third instar larvae of the indicated genotypes. Lack of Fat activity results in overgrown wing discs and increased folding in the proximal wing. (**I**) Adult wing from $fat^{8}/fat^{G\text{-}rv}$ expressing *tub-Gal4 UAS-wts* and *P[acman] V5:fatΔICD[68A4]*.

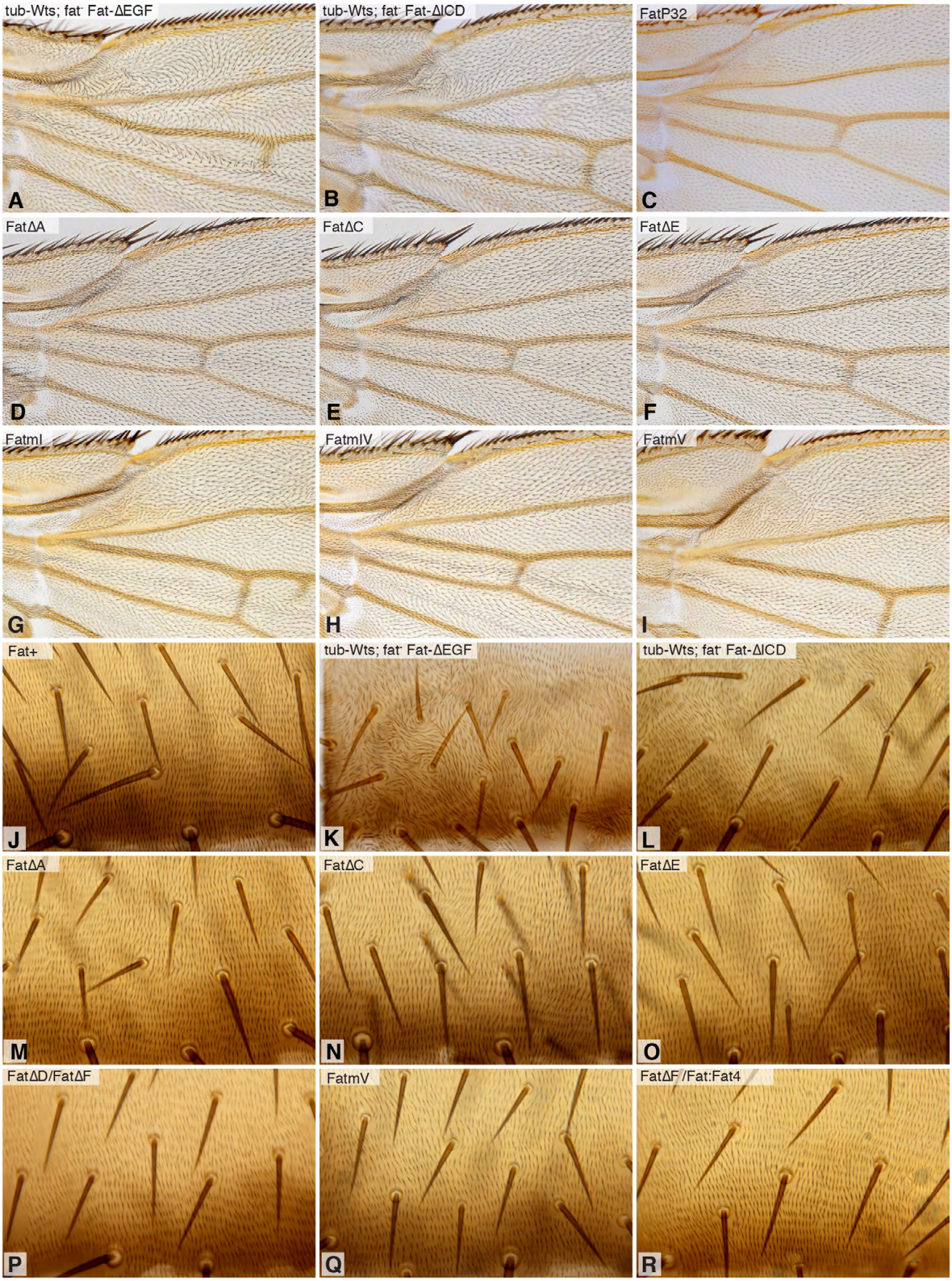

Fig. S3. Additional analysis of hair polarity phenotypes associated with Fat ICD motif mutations. (**A-I**) Proximal anterior wings from $fat^{8}/fat^{G\text{-}rv}$ expressing (A) *tub-Gal4 UAS-wts P[acman]V5:fatΔEGF[68A4],* (B) *tub-Gal4 UAS-wts P[acman]V5:fatΔICD[68A4],* (C) *P[acman]V5:fatP32[68A4]*, (D) *P[acman]V5:fatΔA[68A4],* (E) *P[acman]V5:fatΔC[68A4],* (F) *P[acman]V5:fatΔE[68A4],* (G) *P[acman]V5:fat-mI[68A4],* (H) *P[acman]V5:fat-mIV[68A4],* (I) *P[acman]V5:fat-mV[68A4]*. (**J-R**) Abdomens from $fat^{8}/fat^{G\text{-}rv}$ expressing (J) *P[acman]V5:fat[68A4],* (K) *tub-Gal4 UAS-wts P[acman]V5:fatΔEGF[68A4],* (L) *tub-Gal4 UAS-wts P[acman]V5:fatΔICD[68A4,* (M) *P[acman]V5:fatΔA[68A4],* (N) *P[acman]V5:fatΔC[68A4],* (O) *P[acman]V5:fatΔE[68A4],* (P) *P[acman]V5:fatΔD[68A4]/ P[acman]V5:fatΔF[68A4],* (Q) *P[acman]V5:fat-mV[68A4],* (R) *P[acman]V5:fatΔF[68A4]/P[acman]V5:fat:Fat4[68A4].*

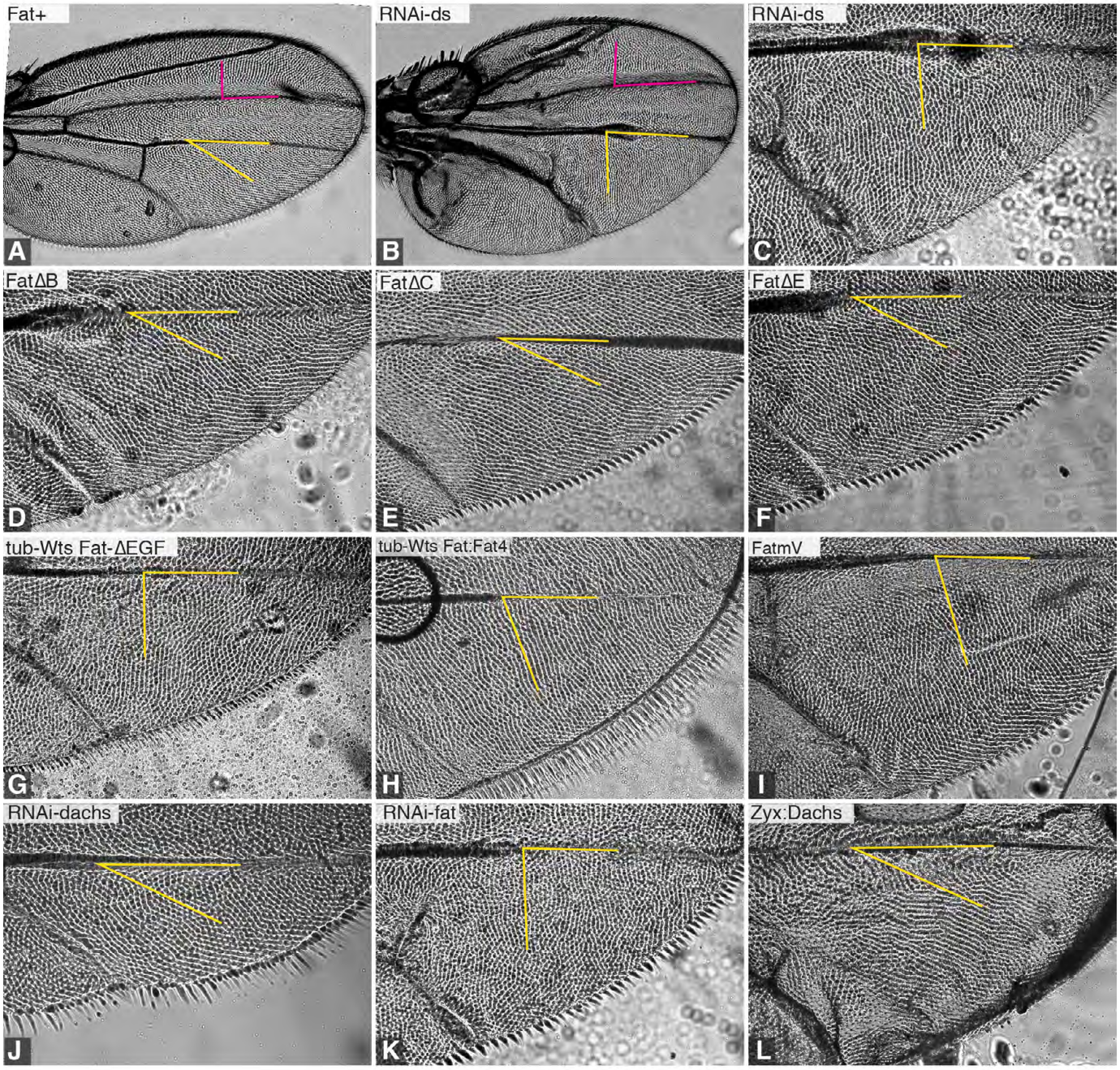

Fig. S4. Additional analysis of ridge polarity. Proximal anterior wings, visualized by cuticle refraction microscopy (Doyle et al., 2008), from $fat^{8}/fat^{G\text{-}rv}$ expressing (**A**) *P[acman]V5:fat[68A4],* (**D**) *P[acman]V5:fatΔB[68A4],* (**E**) *P[acman]V5:fatΔC[68A4],* (**F**) *P[acman]V5:fatΔE[68A4],* (**G**) *tub-Gal4 UAS-wts P[acman]V5:fatΔEGF[68A4],* (**H**) *tub-Gal4 UAS-wts P[acman]V5:fat:Fat4[68A4],* (**I**) *P[acman]V5:fat-mV[68A4],* or from fat^{+} flies expressing *nub-Gal4* and (**B**,**C**) *UAS-RNAi-ds*, (**J**) *UAS-RNAi-dachs*, (**K**) *UAS-RNAi-fat*, (**L**) *UAS-Zyx:dachs*.

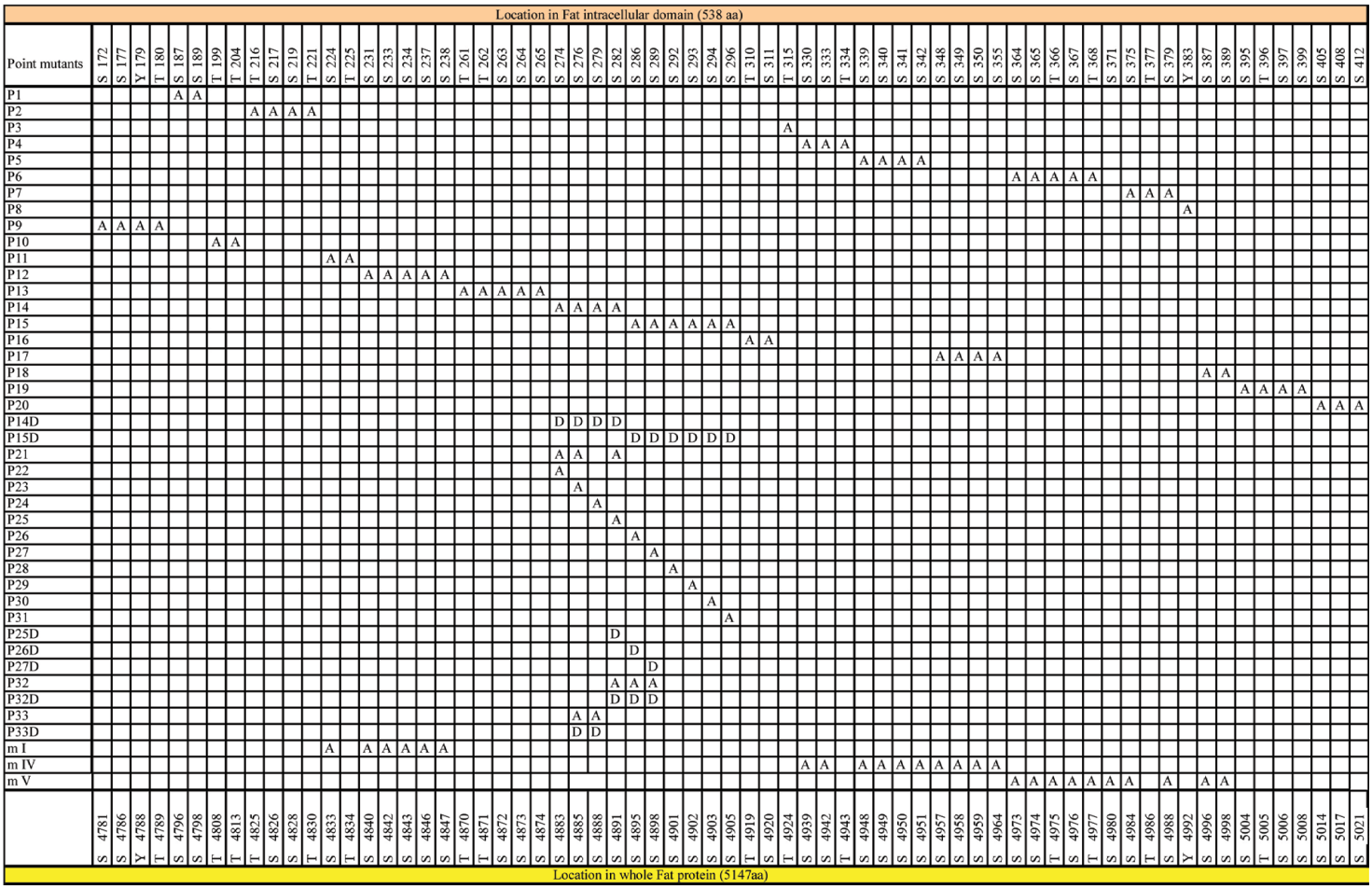

Fig. S5. Potential phosphorylation sites altered in point mutant constructs. Potential phosphorylation sites (Ser, Thr or Tyr) within the Fat intracellular domain were mutated to Ala or Asp, as indicated, within a series of constructs, which were then analyzed for effects on Fat mobility or activity. The first column indicates the name of the construct, top row shows the location of the site within the intracellular domain, bottom row shows location within the entire Fat coding sequence. Middle rows show amino acid mutations within each construct.

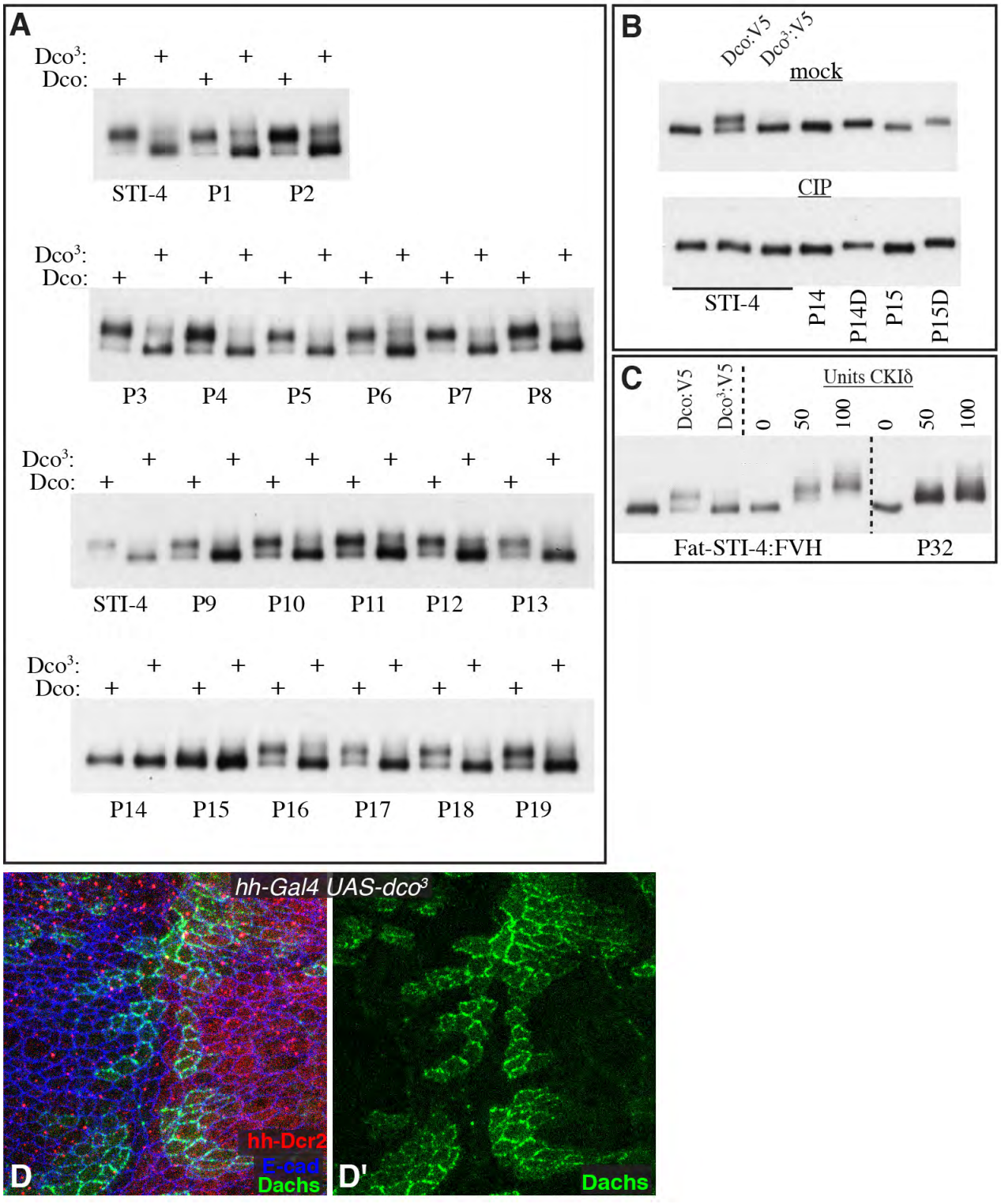

Fig. S6. Additional analysis of Fat ICD phosphorylation. (**A**) Western blots on S2 cell lysates expressing Fat-STI-4:FVH (STI-4) and point mutant derivatives, together with Dco or Dco^3, as indicated. The amino acids mutated in each construct are indicated in Fig. S5. Of the mutants shown here, only P14 and P15 fail to exhibit the Dco-mediated mobility shift. (**B**) The mobility shift induced by Ser to Asp mutations is not reversed by phosphatase treatment (CIP). (**C**) Western blot of products of a kinase assay with vertebrate CKId shows that purified Fat-STI-4:FVH can be directly phosphorylated by CKI *in vitro*, with the extent of phosphorylation proportional to the amount of enzyme; for comparison, protein phosphorylated *in vivo* was run on the same gel. The S-to-A triple mutant Fat-STI-4-P32:FVH is still a substrate for CKId, but the degree of phosphorylation, as assayed by mobility shift, is reduced. (**D**,**D′**) Overexpression of *dco^3* in posterior cells, under *hh-Gal4* control (red), does not affect Dachs:Cit staining (green); Dachs:Cit in anterior cells serves as an internal control. Overexpression of Dco^3 mimics *dco^3* mutation (Feng and Irvine, 2009); this confirms earlier studies of the lack of effect of *dco^3* mutant clones on Dachs localization (Feng and Irvine, 2009).

Table S1. Wing measurement statistics

Rescue constructs	Normalized mean wing area	Standard deviation	Number measured	Standard error of the mean	*P*-value for *t*-test to Fat$^+$
Fat$^+$	1.00	0.030	29	0.006	
FatΔA	0.96	0.034	19	0.008	1.03E–04
FatΔB	1.05	0.043	16	0.011	1.65E–04
FatΔC	0.98	0.044	29	0.008	4.52E–02
FatΔD	1.29	0.051	34	0.009	1.23E–33
FatΔE	1.08	0.043	37	0.007	3.34E–13
FatΔF	1.04	0.057	32	0.010	2.89E–04
FatΔF/FatΔD	1.07	0.037	12	0.011	1.12E–05
FatΔD/FatΔD	1.17	0.042	15	0.011	3.15E–12
FatΔF/FatΔF	0.96	0.068	16	0.017	2.46E–02
Fat$^+$/FatΔD	0.96	0.027	10	0.009	9.53E–04
Fat$^+$/FatΔF	0.94	0.019	10	0.006	1.99E–08
FatΔD/FAT4	1.33	0.029	8	0.010	6.55E–12
FatΔF/FAT4	1.22	0.040	12	0.012	1.02E–11
Fat$^+$/FAT4	0.99	0.028	12	0.008	2.56E–01
FatP32/	1.05	0.029	23	0.006	4.63E–07
FatmI/	1.18	0.036	16	0.009	8.49E–16
FatmIV/	1.08	0.014	12	0.004	5.14E–14
FatmV/	1.35	0.047	28	0.009	1.79E–33
FatmV/FatΔD	1.30	0.034	11	0.010	1.46E–14
FatΔF/FatmV	1.12	0.028	12	0.008	3.73E–11

Rescue constructs	Normalized cross-vein distance	Standard deviation	Number measured	Standard error of the mean	*P*-value for *t*-test to Fat$^+$
Fat$^+$	1.00	0.039	19	0.009	
FatΔA	1.00	0.027	18	0.006	6.53E–01
FatΔB	0.97	0.039	16	0.010	1.27E–02
FatΔC	1.04	0.038	29	0.007	2.07E–04
FatΔD	0.73	0.046	30	0.008	1.41E–31
FatΔE	0.87	0.037	31	0.007	3.17E–20
FatΔF	0.27	0.055	28	0.010	6.78E–45
FatΔF/FatΔD	0.62	0.055	11	0.016	1.28E–11
FatΔD/FatΔD	0.64	0.053	14	0.014	4.21E–15
FatΔF/FatΔF	0.28	0.048	16	0.012	2.92E–26
Fat$^+$/FatΔD	0.94	0.036	10	0.011	4.91E–04
Fat$^+$/FatΔF	0.92	0.037	10	0.012	1.75E–05
FatΔD/FAT4	0.77	0.044	6	0.018	1.26E–05
FatΔF/FAT4	0.66	0.043	7	0.016	5.04E–08

Fat⁺/FAT4	1.03	0.033	12	0.010	2.69E–02
FatP32/	0.97	0.033	23	0.007	1.68E–03
FatmI/	0.77	0.042	14	0.011	1.65E–14
FatmIV/	1.07	0.040	12	0.012	2.61E–05
FatmV/	0.79	0.065	28	0.012	3.20E–18
FatmV/FatΔD	0.70	0.045	7	0.017	2.93E–07
FatΔF/FatmV	0.63	0.053	9	0.018	1.71E–09

Rescue Constructs	Normalized width/length ratio	Standard deviation	Number measured	Standard error of the mean	*P*-value for *t*-test to Fat⁺
Fat⁺	1.00	0.009	29	0.002	
FatΔA	0.99	0.008	18	0.002	1.83E–02
FatΔB	1.01	0.007	16	0.002	2.31E–07
FatΔC	1.00	0.012	26	0.002	9.87E–02
FatΔD	1.16	0.016	30	0.003	2.38E–42
FatΔE	1.05	0.013	31	0.002	1.94E–24
FatΔF	1.12	0.025	31	0.004	5.05E–26
FatΔF/FatΔD	1.12	0.010	12	0.003	6.85E–19
FatΔD/FatΔD	1.12	0.010	12	0.003	3.21E–15
FatΔF/FatΔF	1.18	0.021	14	0.006	1.57E–14
Fat⁺/FatΔD	1.12	0.021	16	0.005	5.05E–05
Fat⁺/FatΔF	1.02	0.010	9	0.003	4.89E–09
FatΔD/FAT4	1.02	0.006	10	0.002	5.12E–10
FatΔF/FAT4	1.18	0.016	8	0.006	1.84E–09
Fat⁺/FAT4	1.19	0.014	7	0.005	1.13E–08
FatP32/	1.01	0.003	12	0.001	1.93E–04
FatmI/	1.15	0.013	16	0.003	4.73E–24
FatmIV/	0.99	0.007	12	0.002	1.85E–03
FatmV/	1.25	0.024	26	0.005	4.78E–32
FatmV/FatΔD	1.19	0.026	10	0.008	6.76E–10

The normalized width/length ratio was calculated by measuring the width and length as indicated in the image below, and then normalizing to the average value in wild-type wings.

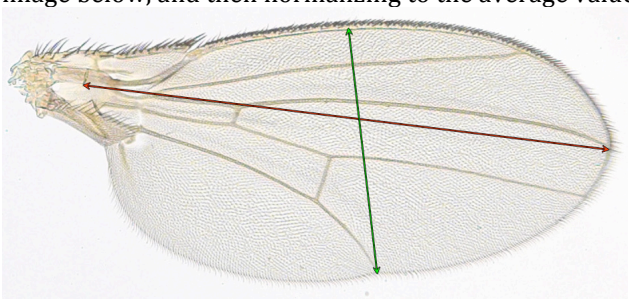

Table S2. Primers

Primers to generate Fat ICD truncates in pUAST-fat plasmid

Construct	PCR template	Primers for 5' fragment		Primers for middle fragment		Primers for 3' fragment	
ft-STI	ft:FVH	ftSPL_NotI5	ftSPL_SOE3			ftL2_SOE5	ftFVH_XbaI3
ft-STI-1	ft-STI	ftSPL_NotI5	STI-1-SOE			FVH_SOE5	ftFVH_XbaI3
ft-STI-2	ft-STI	ftSPL_NotI5	STI-2-SOE			FVH_SOE5	ftFVH_XbaI3
ft-STI-3	ft-STI	ftSPL_NotI5	STI-3-SOE			FVH_SOE5	ftFVH_XbaI3
ft-STI-4	ft:FVH	ftSPL_NotI5	STI-4-SOE			TM-SOE	ftFVH_XbaI3
ft-STI-5	ft-STI	ftSPL_NotI5	ft-TM3	STI5-SOE-A	STI5-SOE-B	FVH_SOE5	ftFVH_XbaI3
ft-STI-6	ft-STI	ftSPL_NotI5	ft-TM3	STI6-SOE-A	STI-2-SOE	FVH_SOE5	ftFVH_XbaI3
ft-STI-7	ft-STI	ftSPL_NotI5	ft-TM3	STI7-SOE-A	STI-3-SOE	FVH_SOE5	ftFVH_XbaI3
ft-STI-8	ft-STI	ftSPL_NotI5	ft-TM3	STI8-SOE-A	STI8-SOE-B	FVH_SOE5	ftFVH_XbaI3
ft-STI-9	ft-STI	ftSPL_NotI5	ft-TM3			STI9-SOE	ftFVH_XbaI3
ft-STI-10	ft-STI	ftSPL_NotI5	ft-TM3	STI5-SOE-A	STI-3-SOE	FVH_SOE5	ftFVH_XbaI3
ft-STI-11	ft-STI	ftSPL_NotI5	ft-TM3	STI6-SOE-A	STI-3-SOE	FVH_SOE5	ftFVH_XbaI3
ft-STI-12	ft-STI	ftSPL_NotI5	ft-TM3			STI5-SOE-A	ftFVH_XbaI3
ft-STI-13	ft-STI	ftSPL_NotI5	ft-TM3			STI6-SOE-A	ftFVH_XbaI3
ft-STI-14	ft-STI	ftSPL_NotI5	ft-TM3			STI7-SOE-A	ftFVH_XbaI3
ft-STI-15	ft-STI	ftSPL_NotI5	ft-TM3			STI8-SOE-A	ftFVH_XbaI3

Primer sequences

ftSPL_NotI5: 5’-TCT GCG GCC GCA TGG AGA GGC TAC TGC TCC-3’

ftSPL_SOE3: 5’-TGA AGT TGA GAG TGC TTC TTC TTC GCG GAA AGG CGG CAT-3’

ftL2_SOE5: 5’-CCG CGA AGA AGA AGC ACT CTC AAC TTC AAC AAA CAG CCC CTG-3’

ftFVH_XbaI3: 5’-GG TCT AGA GAT CA GCG GGT TTA AAC TCA ATG GTG-3’

FVH_SOE5: 5’-ACC GAC TAC AAG GAC GAC GAC GAC AAG-3’

(Overlapping sequence: 5’-CGT CGT CGT CCT TGT AGT CGG TAC C-3’)

STI-1-SOE: 5’- CGT CGT CGT CCT TGT AGT CGG TAC C AAG CGG CGG AAT GGG CAG GTG ATG-3’

STI-2-SOE: 5’- CGT CGT CGT CCT TGT AGT CGG TAC C TTC GCT GTT GCT GTG AAC GTC CTT-3’

STI-3-SOE: 5’- CGT CGT CGT CCT TGT AGT CGG TAC C CTC ACC ACC GCT TAG TGC TCT GGA-3’

STI-4-SOE: 5’-CTT CTT CGC GGA AAG GCG GCA TAT-3’

TM-SOE: 5’-GCC GCC TTT CCG CGA AGA AGA GCC GAT CCT CTC AGC ATT GGC TTC-3’

ft-TM3: 5’-CGA TAG ATA ACA TAG GAG CCC AGT-5’

(Overlapping sequence: 5’-GGG CTC CTA TGT TAT CTA TCG ATT C-3’)

STI5-SOE-A: 5’- GGG CTC CTA TGT TAT CTA TCG ATT C CAG CAA CGT CCC CAG CGA CCC GAT-‘3

STI6-SOE-A: 5’- GGG CTC CTA TGT TAT CTA TCG ATT C AGT GTT CCA CCT GTT TCC GCC

TAC-3’

STI7-SOE-A: 5’- GGG CTC CTA TGT TAT CTA TCG ATT C CAC AGC AAC AGC GAA CGC AGT CTG-3’

STI8-SOE-A: 5’- GGG CTC CTA TGT TAT CTA TCG ATT C AAC AGT CTC AGT GGC GAC GGC AAG-3’

STI9-SOE: 5’- GGG CTC CTA TGT TAT CTA TCG ATT C AAT GGA GCC GCA TCC CCA TCG GCC-3’

(Overlapping sequence: 5’-CGT CGT CGT CCT TGT AGT CGG TAC C-3’)

STI5-SOE-B: 5’- CGT CGT CGT CCT TGT AGT CGG TAC C GGC CTT GTA TTT GCG TAG GCC

AGC-3’

STI8-SOE-B: 5’- CGT CGT CGT CCT TGT AGT CGG TAC C ATT GGC CTT GCG GTA GAT ACC GCT C-3’

Primers to generate human Fat-ICD and *Drosophila* Fat hybrid genomic constructs:

1. Forward: galK_ICD_F: ATT GTC TTC TTC GTC ATT CTG GTG GTG GCT ATA CTG GGC TCC TAT GTT ATC TAT CGA

TTC CCT GTT GAC AAT TAA TCA TCG GCA

1. Reverse: galK_ICD_R:

TGG GGC TCA GAC TTT AGG AAC ACT TTA ACT TTC GTT GAA GAG CAT ACA CAA CAT ATA TTA TCA GCA CTG

TCC TGC TCC TT

2. hsft4_SOE5: GGG CTC CTA TGT TAT CTA TCG ATT C AAC CAG TGC AGG GGG AAG AAG

GCC

2. hsft4_FLAGXhoI3: AAA CTC GAG TCA ACC CTT GTC GTC GTC GTC CTT GTA GTC CAC ATA

3. TM_F: CTCAGCATTGGCTTCACCCTGGTC

3. TM_R: CGATAGATAACATAGGAGCCCAGT

3. FLAGft_dwn_F: GAC TAC AAG GAC GAC GAC GAC AAG GGT TGA TA ATA TAT GTT GTG TAT GCT CTT CAA CG

3. FLAG_R: TCA ACC CTT GTC GTC GTC GTC CTT GTA GTC

Notes: 1. Primers used to insert galK into fly fat ICD region. 2. Primers used to generate fusion protein of human Fat-ICD with *Drosophila* Fat (signal peptide plus transmembrane domain) in pUAST plasmid. 3. Primers used to generate fusion proteins of human Fat-ICD with *Drosophila* Fat (ECD plus transmembrane domain) in genomic rescue construct

Primers to generate *fat* genomic rescue constructs with deletions:

A. Fat-Delta aa4704-4711-Fgalk: GAACCCACTGCGGAGATGCCACAGCCGCAGCAGCAGCAGCAACGTCCCCAG

CCTGTTGACAATTAATCATCGGCA

A. Fat-Delta aa4704-4711-Rgalk: GGATGAAGCGGCGGAATGGGCAGGTGATGATCCTCCCTTATCAGAGGACT

TCAGCACTGTCCTGCTCCTT

A. Fat ICD F: ATTGTCTTCTTCGTCATTCTGGTGGTGGCTATACTGGGCTCCTATGTTATCTATCGATTC

A. FatDel4704-4711R: GATCCTCCCTTATCAGAGGACTCTGGGGACGTTGCTGCTGCTGC

A. FatDel4704-4711F: GCAGCAACGTCCCCAGAGTCCTCTGATAAGGGAGGATCATC

A. FatDel4921-4959R: GGAAGTTTGCTGCGCCTGCTGCT

B. Fat-Delta aa4745-4770-Fgalk:CTCTCCCGCTGGAGCACGCCAGTTCCGTGGACATGGGTTCCGAGTACCCG

CCTGTTGACAATTAATCATCGGCA

B. Fat-Delta aa4745-4770-Rgalk:

GCGGAAACAGGTGGAACACTGGCCTTGTATTTGCGTAGGCCAGCAGCCTC TCAGCACTGTCCTGCTCCTT

B. Fat ICD F FatDel4745-4770R: TGCGTAGGCCAGCAGCCTCCGGGTACTCGGAACCCATGTCC

B. FatDel4745-4770F: GACATGGGTTCCGAGTACCCGGAGGCTGCTGGCCTACGCAAATA

B. FatDel4921-4959R: GGAAGTTTGCTGCGCCTGCTGCT

C. Fat-Delta aa4921-4959-Fgalk:CCAGCAGGCAAAAGCCCGGAGTGCCACAGCAGCAGGCGCAGCAAACTTCC

CCTGTTGACAATTAATCATCGGCA

C. Fat-Delta aa4921-4959-Rgalk:GAAGTCGAACTATGGGCATCCACATCTCCACCCAGCGACATATGCAGAGC

TCAGCACTGTCCTGCTCCTT

C. ftSTm_checkF:GCCAGTTCCGTGGACATGGGTTCC

C. FatDel4921-4959R: GGAAGTTTGCTGCGCCTGCTGCT

C. FatDel4921-4959F:TGCCACAGCAGCAGGCGCAGCAAACTTCCGCTCTGCATATGTCGCTGGGTGGA

C. ftSTm_checkR:cggaatgggcggtgtcttgaccac

D. Fat-Delta aa4975-4993-Fgalk:GCAGCGCTCTGCATATGTCGCTGGGTGGAGATGTGGATGCCCATAGTTCG CCTGTTGACAATTAATCATCGGCA

D. Fat-Delta aa4975-4993-Rgalk:GAGGAGACTCTTGCTGGTGGAATACTTGCCGTCGCCACTGAGACTGTTATT TCAGCACTGTCCTGCTCCTT

D. ftSTm_checkF: FatDel4975-4993R: GCCGTCGCCACTGAGACTGTTATTCGAACTATGGGCATCCACATCTCCA

D. FatDel4975-4993F: GAGATGTGGATGCCCATAGTTCGAATAACAGTCTCAGTGGCGACGGCA

D. ftSTm_checkR

E. Fat-Delta aa5089-5114-Fgalk:TCTACCGCAAGGCCAATGGAGCCGCATCCCCATCGGCCACCACCCTCGGC CCTGTTGACAATTAATCATCGGCA

E. Fat-Delta aa5089-5114-Rgalk:GTGGACACCACTTGGGTTTGCTGCTGCTGTTGCTGCGACGGTCCATTTGT TCAGCACTGTCCTGCTCCTT

E. Fat-DeltaCDEseq-F: GCAAGGACGTTCACAGCAACAGCG

E. FatDel5089-5114R: GTTGCTGCGACGGTCCATTTGTGCCGAGGGTGGTGGCCGATGGGGA

E. FatDel5089-5114F: CATCGGCCACCACCCTCGGCACAAATGGACCGTCGCAGCAACA

E. FLAG_R:TCAACCCTTGTCGTCGTCGTCCTTGTAGTC

F. Fat_Cterm_galkF: GTG GTG TCC ACG CTA CGA ATG CCA TCA TCG AAT GGA CCG GCG GCT CCA GAG GAG TAC GTG CCT GTT GAC AAT TAA TCA TCG GCA

F. Fat_Cterm_galkR: TGG GGC TCA GAC TTT AGG AAC ACT TTA ACT TTC GTT GAA GAG CAT ACA CAA CAT ATA TTA TCA GCA CTG TCC TGC TCC TT

F. Fat-HomoDomainF-F:GACTACAAGGACGACGACGACAAGGGTTGA

F. Fat_C_chckR:TCCGACATATGCACGATTCTACAC

EGF. Fat-EGF1flank-Fgalk:GAGAGAAGCGTTCAGCGTTTTCGGAACTCCTGCAAAAGGAGGTGATTGTG

CCTGTTGACAATTAATCATCGGCA

EGF. Fat-EGF4flank-Rgalk:GAGCGGGAAAAGTCATGTAGGACAGCGGTTGGAATCCATAGCTAAAACG

TCAGCACTGTCCTGCTCCTT

EGF. Fat33759seq_F: AGAATCCCGCCCAGAGTCAA

EGF. FatDelEGF1-4R: GGAATCCATAGCTAAAACGCACAATCACCTCCTTTTGCA

EGF. FatDelEGF1-4F: GCAAAAGGAGGTGATTGTG CGTTTTAGCTATGGATTCCAA

EGF. Fat34583seq_R: GGTCCCACTTCGTCCGCATA

Notes: Deletions were created by first replacing the relevant region with *galK*. The forward fragment and reverse fragments were then hybridized and extended to generate a DNA fragment without the relevant region but both 5' and 3' homolog arms for recombineering. Primers listed were: (A) for deletion of region A (RPDIIERE, aa4704-4711, cgacccgatatcatagagcgcgag), creating plasmid *attB-P[acman]-V5ftΔA-Flag*; (B) for deletion of region B (EHYDLENASSIAPSDIDIVYHYKGYR, aa4745-4770, gaacactacgacctcgagaacgccagctccattgctccgtccgacattgatatagtctatcattacaagggctatcgt), creating plasmid *attB-P[acman]-V5ftΔB-Flag*; (C) for deletion of region C (MGLTAEEIERLNGRPRTCSLISTLDAVSSSSEAPRVSSS, aa4921-4959, atgggcttgaccgccgaggagattgagagattgaatggcagaccacgaacttgtagcctaatctccaccctggatgccgtctcctccagcagtgaggcgcctcgagtgtcgagcagc), creating plasmid *attB-P[acman]-V5ftΔC-Flag*; (D) for deletion of region D (TSTDESGNDSFTCSEIEYD, aa4975-4993, acttccacggacgaaagcggcaacgacagcttcacgtgctcggagatcgagtacgac), creating plasmid *attB-P[acman]-V5ftΔD-Flag*; (E) for deletion of region E (WEYLLNWGPSYENLMGVFKDIAELPD, aa5089-5114, tgggagtatctgctcaattggggacctagctacgaaaatctgatgggcgtcttcaaggacattgccgagctgccggac), creating plasmid *attB-P[acman]-V5ftΔE-Flag*; (F) For deletion of region F (EEYV, aa5144-5147, gaggagtacgtg), creating plasmid *attB-P[acman]-V5ftΔF-Flag*; (EGF) for deletion of region EGF (GYEPCSEPDVCENGGVCSATMRLLDAHSFVIQDSPALVLSGPRVVHDYSCQCTSGFSGEQCSRRQDPCLPNPCHSQVQCRR LGSDFQCMCPANRDGKHCEKERSDVCYSKPCRNGGSCQRSPDGSSYFCLCRPGFRGNQCESVSDSCRPNPCLHGGLCVSLKP GYKCNCTPGRYGRHCE, aa3950-4128, ggctatgaaccctgcagtgaaccggatgtttgtgaaaatggcggagtctgcagtgccaccatgcgactgctggatgcccatagctttgttatccaagacagtccggccttggtgctgagtggtcctcg ggttgtgcacgactacagctgccagtgcaccagtggattctcgggcgagcagtgcagtcgtcggcaggatccttgcctgcccaatccttgccattcgcaggtccaatgccgtcgcctgggtagcgat ttccagtgcatgtgtcctgccaatcgggatggcaagcactgcgagaaggaacgcagtgacgtgtgctatagcaagccgtgtcgcaatggaggaagttgccaacgcagtccggacggatcctccta

cttttgcctatgtcgtcccggattccgtggcaatcagtgcgagagcgtgtcggactcatgccgacccaatccctgtctgcacggtggcttgtgtgttagtctcaagccaggatacaaatgcaactgcac gccgggacgatatggacgacattgcgag), creating plasmid *attB-P[acman]-V5ftΔEGF-Flag*.

Primers to generate *fat* genomic rescue constructs with deletions:

fatmutrecgalKI-F: AAGGTGGCCAACCGCCACCGCCGCCCACCAGTGCATCCCGCACCCATCAG

CCTGTTGACAATTAATCATCGGCA

fatmutrecgalKVI-R:

CCATTGGCCTTGCGGTAGATACCGCTCAGGTGATTGGCTATATCATCGTC TCAGCACTGTCCTGCTCCTT

I-F: GCA TCC CGC ACC CAT CAG GCC ACT CCA CTG GCC CGA CTC

IV-F: GGC AGA CCA CGA ACT TGT GCC CTA ATC GCC ACC CTG GAT GCC GTC GCC

IV-R: GAG GCG CCT CGA GTG GCG GCC GCC GCT CTG CAT ATG GCG CTG GGT GGA GAT GTG

V1-F: GCT GCC GCG GAC GAA GCC GGC AAC GAC AGC TTC

V1-R: GAG TAC GAC AAT AAC GCT CTC GCT GGC GAC GGC AAG TAT

V-R: GAA GCC GGC AAC GAC GCC TTC ACG TGC GCG GAG ATC GAG TAC GAC

fatmutrecI-F: AAGGTGGCCAACCGCCACCGCCGCCCACCAGTGCATCCCGCACCCATCAG

fatmutrecVI-R: CCATTGGCCTTGCGGTAGATACCGCTCAGGTGATTGGCTATATCATCGTC

Notes: First, the sequence between Fat-mI and Fat-mV was replaced by *galK* using fatmutrecgalKI-F and fatmutrecgalKVI-R to generate plasmid *attB-P[acman]-V5ft-mut-galK-Flag*. Then, nucleotide substitutions were introduced into pUAST-fat-STI plasmid, using I, IV, or V primers to generate pUAST-fat-mutI, pUAST-fat-mutIV and pUAST-fat-mutV. The mutated fragments were PCR amplified from pUAST-fat-mutI, pUAST-fat-mutIV and pUAST-fat-mutV and introduced into *attB-P[acman]-V5ft-mut-galK-Flag* to generate plasmids *attB-P[acman]-V5ft-mutI-Flag*, *attB-P[acman]-V5ft-mutIV-Flag*, *attB-P[acman]-V5ft-mutV-Flag.*

Primers to introduce the ΔD and mV mutations into pUAST_ft_STI4FVH construct:

Fat-STI:4- ΔD:FLAG (pUAS_ft_STI4_ ΔD _FVH)

Fat-STI:4- mutV:FLAG (pUAS_ft_STI4_mutV_FVH)

STI4FVH_ deleteD_F: GATGTGGATGCCCATAGTTCGAATAACAGTCTCAGTGGCGAC

STI4FVH_ deleteD_R: GTCGCCACTGAGACTGTTATTCGAACTATGGGCATCCACATC

Notes: The ΔD or mV mutation was amplified by PCR from corresponding genomic constructs. Then these PCR fragments were introduced into the pUAST_ft_STI4FVH plasmid.

Table S3. Abbreviations for Fat transgenes

Abbreviated name	Full name
Fat⁺	*P[acman]V5:fat[68A4]*
FatΔA	*P[acman]V5:fatΔA[68A4]*
FatΔB	*P[acman]V5:fatΔB[68A4]*
FatΔC	*P[acman]V5:fatΔC[68A4]*
FatΔD	*P[acman]V5:fatΔD[68A4]*
FatΔE	*P[acman]V5:fatΔE[68A4]*
FatΔF	*P[acman]V5:fatΔF[68A4]*
FatΔP32	*P[acman]V5:fat-P32[68A4]*
FatΔmI	*P[acman]V5:fat-mI[68A4]*
FatΔmIV	*P[acman]V5:fat-mIV[68A4]*
FatΔmV	*P[acman]V5:fat-mV[68A4]*
Fat:Fat4	*P[acman]V5:fat:FAT4[68A4]*
FatΔEGF	*P[acman]V5:fatΔEGF[68A4]*